1.E.1:
1.E.3:
3.A:3.B

Nuclear Physics **A159** (1970) 113—142;

LEVEL STRUCTURE OF ^{101}Rh FROM THE DECAY OF 8.5 h ^{101}Pd

MICHAEL E. PHELPS and DEMETRIOS G. SARANTITES
Department of Chemistry, Washington University, St. Louis, Missouri 63130

Received 12 June 1970

Abstract: The level structure of ^{101}Rh has been investigated from the decay of 8.5 h ^{101}Pd. Singles γ-ray energy and intensity measurements were taken with a 25 cm^3 high-resolution Ge(Li) detector in an anti-Compton arrangement which employed a large NaI(Tl) annular detector. Extensive $\gamma\gamma$ coincidence measurements were made with a Ge(Li)–Ge(Li) and a NaI-Ge(Li) arrangement with the Ge(Li) detector under Compton suppression. Triple $\gamma\gamma\gamma$ coincidence measurements were taken in a NaI-Ge(Li)-NaI arrangement with the Ge(Li) detector under Compton suppression. The low-energy γ-rays and X-rays were studied with a high-resolution Si(Li) X-ray spectrometer. Conversion electron measurements were made with Si(Li) detectors and α_K values were determined for the most intense transitions. From these data it was concluded that levels at 157.32, 181.78, 305.3, 355.14, 478.00, 747.67, 905.61, 974.7, 978.42, 1035.5, 1057.7, 1320.4, 1359.31, 1470.82, 1696.27, 1789.26, 1820.22 and 1911.23 keV are populated in the decay of 8.5 h ^{101}Pd. From log *ft* and α_K values determined in this work and from γ-ray intensity information definite J^π assignments were made to a number of levels and limits for the J^π values were placed for the rest of the levels in ^{101}Rh. The fraction of decay of the 4.5 d isomeric state by an isomeric transition was measured to be 0.072 ± 0.004. The level structure and the level trends in the ^{99,101,103,105}Rh isotopes are examined and discussed in relation to recently published results on calculated levels in these isotopes on the basis of an extended pairing-plus-quadrupole model for the nucleus.

E RADIOACTIVITY ^{101}Pd; measured E_γ, I_γ, I_{ce}, K/(L+M), α_K, $\gamma\gamma$-coin, $\gamma\gamma\gamma$-coin; deduced log *ft*. ^{101}Rh deduced levels, cc, γ-multipolarity, J, π. NaI(Tl), Ge(Li), NaI(Tl)–Ge(Li) anti-Compton, Si(Li) electron, Si(Li) X-ray detectors.

1. Introduction

The positon decay of 8.5 h ^{101}Pd has been studied by Lindner and Perlman [1]) who reported a maximum positon energy of 2.3 MeV, and by Eggen and Pool [2]) who reported a maximum positon energy of 0.53 MeV. Katcoff and Abrash [3]) reported a maximum β^+ energy of 0.58 ± 0.08 MeV and γ-rays at 288, 590, 720, 1190 and 1280 keV following decay of 8.5 h ^{101}Pd, with some $\gamma\gamma$ coincidence information between these γ-rays. Thorne and Kashy [4]) studied the levels in ^{101}Rh by the ^{103}Rh(p, t)^{101}Rh reaction and proposed a decay scheme in clear contradiction with that suggested by the Nuclear Data group [5]). At about the same time Dzhelepov *et al.* [6]) proposed an elaborate decay scheme for ^{101}Pd on the basis of singles conversion electron measurements utilizing a magnetic spectrometer and a NaI(Tl)

† Work supported in part by the US Atomic Energy Commission under Contract Nos. AT(11-1)-1530 and AT(11-1)-1760.

γ-ray detector. Another independent and considerably more careful study of the decay of ^{101}Pd was reported by Evans *et al.* [7]) who utilized a high-resolution magnetic spectrometer, NaI(Tl) and Ge(Li) γ-ray detectors. The decay scheme proposed by Evans *et al.* [7]) differs considerably from that of Dzhelepov *et al.* [6]). Apart from the inconsistencies in the decay schemes reported in the literature for ^{101}Pd, the study of the level structure in $^{101}_{45}Rh_{56}$ is of considerable theoretical interest in a serious effort to understand the properties of the low-lying $\frac{5}{2}^+$, $\frac{7}{2}^+$ and $\frac{9}{2}^+$ states in nuclei with Z or N equal to 43, 45 and 47. In a recent paper [8]) we have presented a comparison of the level structure of the ^{99,101,103}Rh isotopes with the predictions of recent theoretical models, such as the pairing-plus-quadrupole model for the nucleus as treated by Kisslinger and Sorensen [9]), the attempts of Ikegami and Sano [10]) to include higher shell admixtures, and the extended quasiparticle-phonon coupling theory (EQPC) of Sherwood and Goswami [11]). A more recent calculation by Goswami and Nalcioglu [12]) based effectively on the EQPC theory, incorporated the large negative quadrupole moment of the 2^+ phonon state of the underlying core and appeared to explain the rather large splitting of the $\frac{5}{2}^+$ and $\frac{7}{2}^+$ states in ^{101}Rh.

The present investigation was undertaken because it was believed that with the improvement in resolution and efficiency of the Ge(Li) detectors a thorough study of the ^{101}Pd decay could be made. The definite characterization of the positive parity states in ^{101}Rh is necessary in order to determine the trend of the individual states in the odd-mass Rh isotopes from $A = 99$ to 105 and thus demonstrate the effect of adding pairs of neutrons on the position of the levels. A comparison of this type with the level trends in the even Ru isotopes, which form the underlying core for the Rh structure was considered instructive.

2. Experimental procedures

2.1. PREPARATION OF ^{99,101}Pd AND ^{101m}Rh SAMPLES

The ^{101}Pd samples were prepared by the ^{98}Ru(^{4}He, n) and ^{99}Ru(^{4}He, 2n) reactions utilizing 18 MeV ^{4}He ions from the Washington University cyclotron on natural ruthenium metal targets. At this energy small amounts of 4.1 d ^{100}Pd are produced by the ^{98}Ru(^{4}He, 2n) reaction ($Q = -17.6$ MeV). In all cases, the following radiochemical procedure was employed in order to purify the Pd activity from the Rh and Ru activities that are produced in substantial yield. Four hours were allowed to elapse after bombardment for the 21 min ^{99}Pd to decay and the Ru metal targets were then dissolved by an alkaline fusion with KOH-KNO_3 (2.5–3.0 g each) at 300 °C in a covered iron crucible for 30 min. The K_2RuO_4 formed was dissolved in 30 ml of hot water and RuO_4 was distilled into a 6 M NaOH trap by bubbling of chlorine gas and heating. The remaining Cl_2 was then expelled by boiling. To this solution 5 mg each of Rh^{III} and Pd^{II} (omitted for carrier-free sources) carriers were added and Pd^{II} was precipitated by addition of 2 ml of saturated ethanol solution of dimethylglyoxime (DMG). The PdDMG was extracted in 50 ml of chloroform and the

organic phase was washed twice with 50 ml portions of 1N H_2SO_4. The chloroform was then removed by evaporation to dryness and the PdDMG was destroyed by boiling with 5 ml of conc. HNO_3 and evaporating to near dryness. Finally the remaining solution was diluted to 20 ml with distilled water and PdDMG was again precipitated, filtered and mounted for γ-counting.

Carrier-free electron ^{99}Pd and ^{101}Pd sources were prepared by following the above purification procedure without Pd^{II} carrier. After the chloroform extraction the Pd DMG was destroyed by adding 5 ml of conc. HNO_3 and carefully evaporating to dryness. The Pd activity was then dissolved in 2 ml of 0.1 M $(NH_4)_2SO_4$ solution at pH 3 and the Pd was electroplated on a platinum foil. This procedure required approximately 30 min from the end of bombardment to the start of counting. In the case of 21 min ^{99}Pd the sources were prepared by the method of ref. [8]). To accelerate electroplating of the ^{99}Pd activity 1.0 μg of Pd^{II} carrier was added initially to the sample.

Carrier-free sources of Rh were prepared by electroplating on platinum after quantitative removal of the Pd which was extracted in chloroform several times as PdDMG. In some cases γ-ray sources were prepared by adding 5 mg of Rh^{III} carrier and 2 ml of 60 % solution of potassium nitrite to precipitate $K_3Rh(NO_2)_6$, which was filtered, washed and mounted for γ-counting.

2.2. DETECTION EQUIPMENT AND METHODS OF COUNTING

For γ-ray counting, both Ge(Li) and NaI(Tl) detectors were employed. The Ge(Li) detectors had active volumes of 25 and 29 cm^3 with FWHM of 2.6 and 2.8 keV at the 1332 keV line of ^{60}Co, respectively. The 29 cm^3 Ge(Li) detector was employed in an anti-Compton arrangement with a 19.9 cm in diameter by 12.7 cm long annular NaI(Tl) detector. A full description of this system and its calibration has been given elsewhere [13]).

For X-ray counting a 50 $mm^2 \times 5$ mm Ge(Li) detector was used with FWHM of 1.05 keV at the 122 keV line of ^{57}Co. At a later stage a 50 $mm^2 \times 5$ mm deep Si(Li) detector with a cooled FET preamplifier was employed. This Si(Li) X-ray detector had a FWHM of 600 eV at 24 keV.

For conversion electron counting two Si(Li) detectors were employed with 1.0 cm^2 area and depletion depths of 0.5 and 1.0 mm. These detectors had a FWHM of 4.3 keV at the 343 keV K-shell line from a ^{206}Bi source. These Si(Li) detectors were used in conjunction with the 25 cm^3 Ge(Li) detector as a conversion electron spectrometer in an arrangement of reproducible geometry. Spectra of γ-rays and conversion electrons could be recorded simultaneously. This spectrometer was calibrated for absolute electron detection efficiency using standard sources of ^{139}Ce, ^{203}Hg, ^{113}Sn, ^{198}Au and ^{137}Cs with well-known K-shell conversion coefficients and a relative electron standard of ^{206}Bi. A typical electron spectrum of a ^{206}Bi source recorded with the 1 $cm^2 \times 1$ mm Si(Li) detector is shown in fig. 1. The electron efficiency of this detector as a function of electron energy is shown in fig. 2.

For $\gamma\gamma$ coincidence counting the following arrangements were employed: (i) Ge(Li) × Ge(Li) with 25 and 29 cm^3 detectors; (ii) NaI(Tl) × Ge(Li) with a 7.6 × 7.6 cm NaI(Tl) and a 29 cm^3 Ge(Li) detector with the Ge(Li) detector operated in the anti-Compton mode; and (iii) NaI(Tl) × Ge(Li) × NaI(Tl) with two 7.6 × 7.6 cm

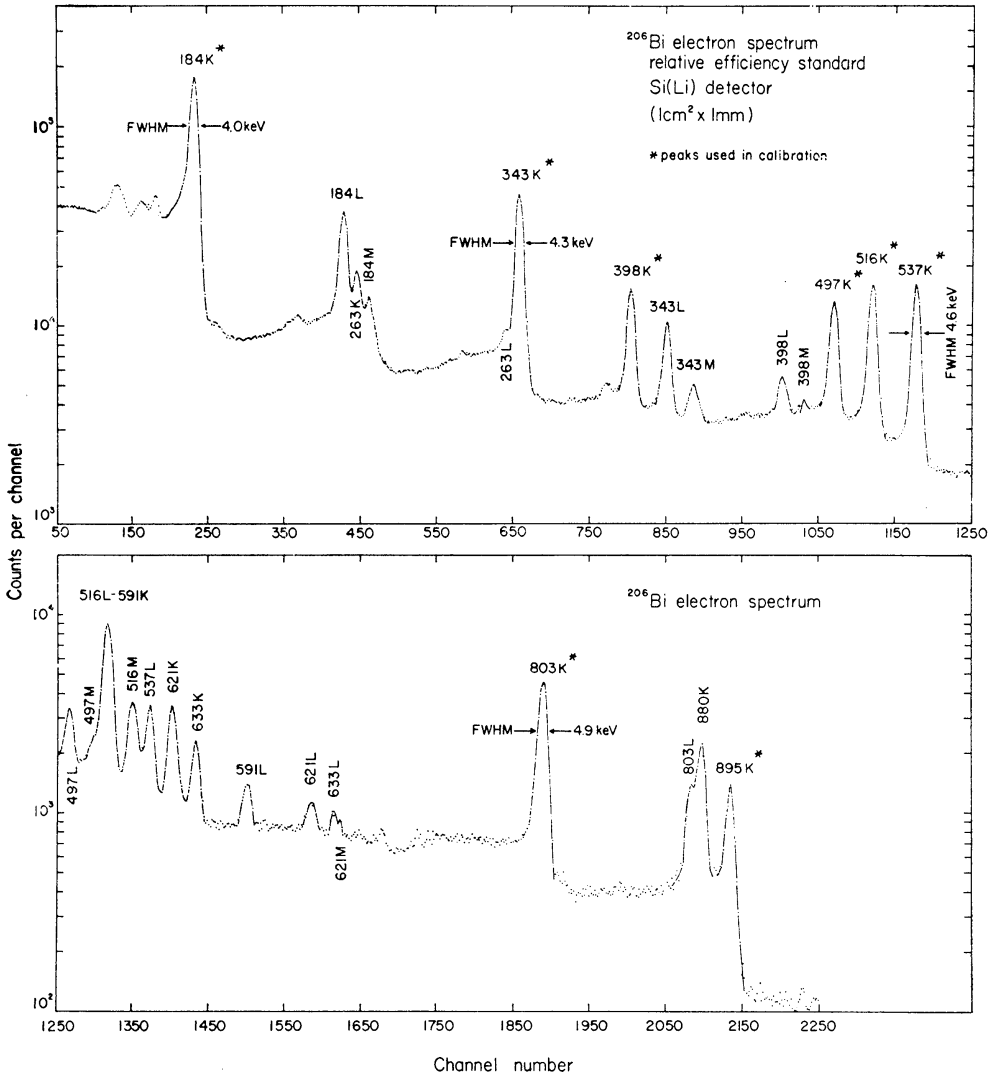

Fig. 1. Typical conversion electron spectrum from a standard ^{206}Bi carrier-free source recorded with a 1.0 cm^2 × 1.0 mm Si(Li) detector. Peaks marked with an asterisk were used in the calibration.

NaI(Tl) detectors and a 29 cm^3 Ge(Li) detector which was operated in the anti-Compton mode (fig. 3). In the double coincidence experiments two parameter spectra in a

256 × 1024 channel configuration for the NaI(Tl) × Ge(Li) or the Ge(Li) × Ge(Li) arrangements were recorded. In the triple coincidence experiments only total coincidence events in the Ge(Li) detector were recorded. In some experiments the source was placed near the Ge(Li) detector and the anticoincidence annulus was not

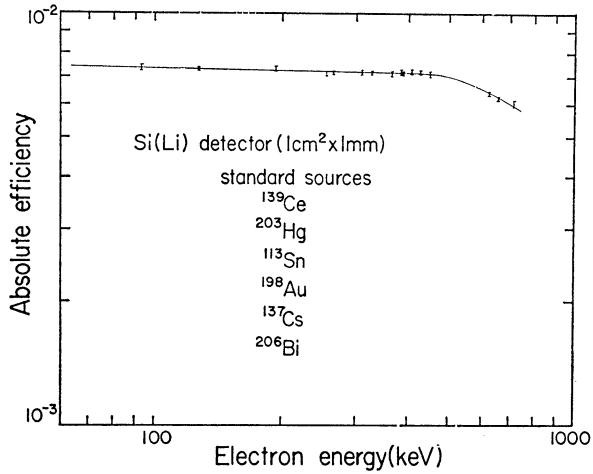

Fig. 2. Absolute efficiency curve of the Si(Li) electron detector in the geometry of the conversion electron spectrometer.

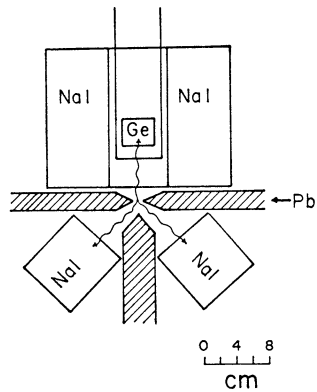

Fig. 3. Detector arrangement employed in the NaI-Ge(Li)-NaI triple coincidence experiments. The annular NaI detector was operated in the anti-Compton mode with respect to the Ge(Li) detector.

shielded from the source. This resulted in suppression of the true coincidence events thus depicting the transitions that populate the ground, the metastable or the 181.78 keV state (the 24.46 keV γ-ray was absorbed by a Cu absorber wrapped around the source).

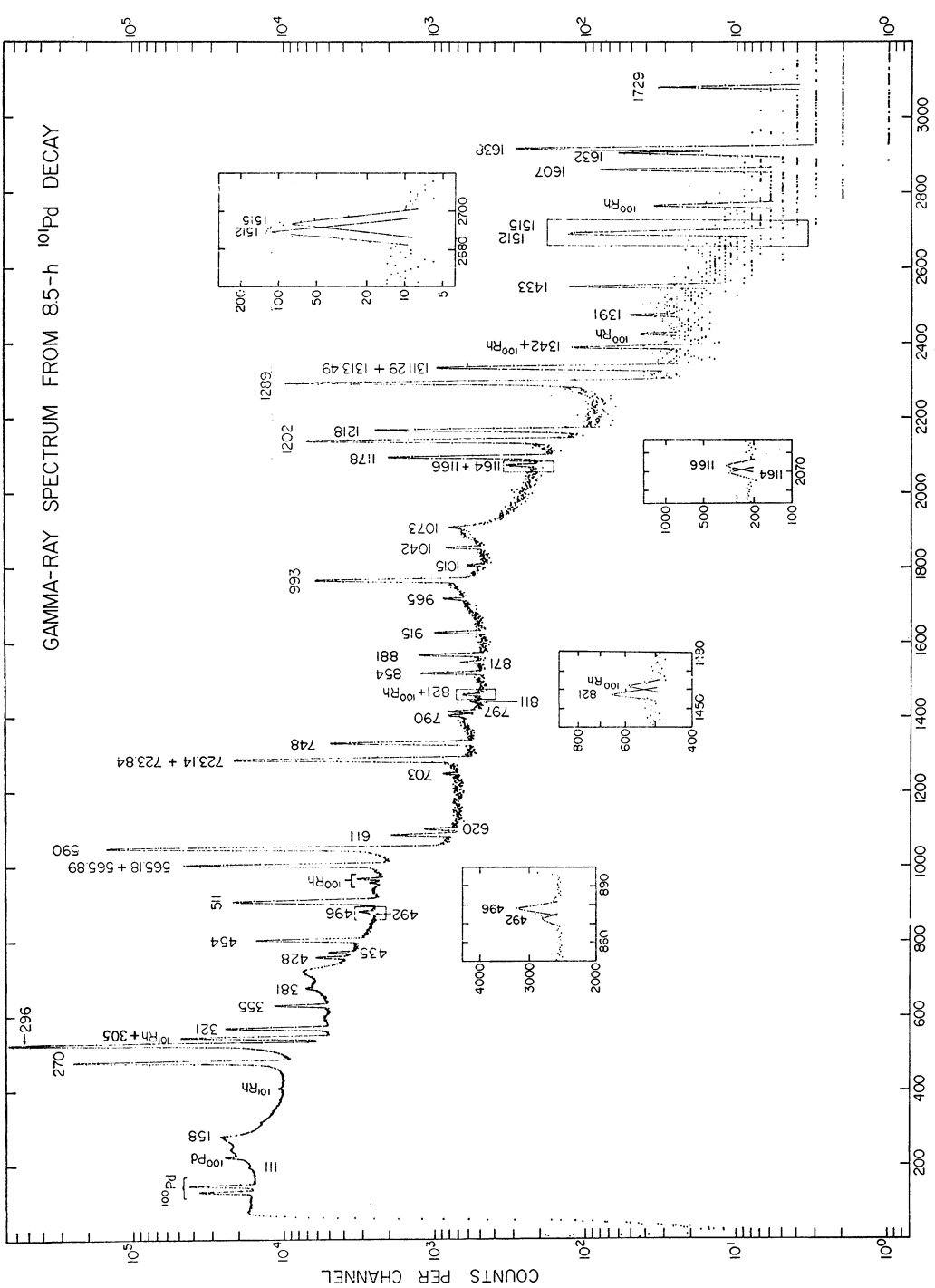

Fig. 4. Typical Compton-suppressed spectrum of the γ-rays following ^{101}Pd decay. Doublets that could be resolved partially are shown in the inserts. Seven additional doublets have been identified (see text) which are too close to show a broadening and are so indicated in the figure.

For pulse-height analysis a 4096-channel two-parameter pulse-height analyzer was employed. This system has been described in some detail in ref. [14]). The random events were determined with the aid of a 60 Hz pulser introduced in one of the preamplifiers as described in ref. [15]). The random events were found negligible and they were not subtracted from the illustrations. Coincidence events resulting from the Compton events of higher energy γ-transitions were taken into account by taking coincidence spectra on either side of each gated γ-peak.

The coincidence spectra presented here from the Ge(Li) × Ge(Li) experiments were obtained by adding the coincidence planes to obtain 9 or 18 keV per channel window in the 25 cm^3 Ge(Li) detector with the aid of a read-search unit.

3. Results

A typical singles Compton suppressed γ-ray spectrum from a source of 8.5 h ^{101}Pd is shown in fig. 4. This spectrum was recorded for a period of 8 h beginning immediately after purification. Subsequent spectra were taken for 72 h in order to identify the

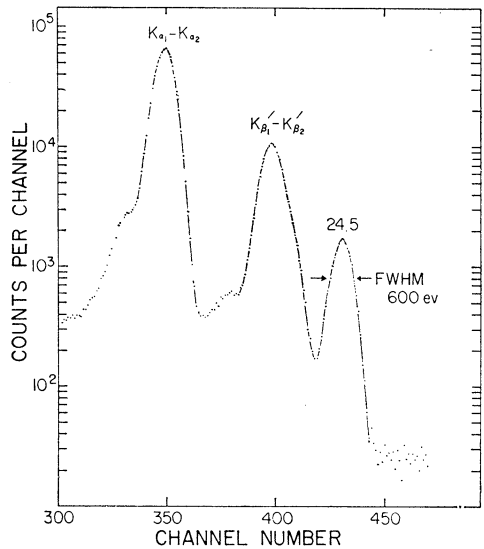

Fig. 5. Typical low-energy spectrum showing the ^{101}Rh x-rays following ^{101}Pd decay. The 24.46 keV γ-ray from ^{101}Pd decay is also clearly seen.

γ-rays by half-life. In the spectrum of fig. 4 the only contaminating γ-rays are due to small amounts of 4.1 d ^{100}Pd, 21 h daughter ^{100}Rh and 4.5 d daughter ^{101}Rh. Fig. 5 shows a spectrum of the ^{101}Rh X-rays following ^{101}Pd decay. This spectrum was taken with a Si(Li) X-ray detector and shows the 24.46 keV γ-ray from ^{101}Pd decay.

TABLE 1

Energy and relative intensity of the γ-rays following ^{101}Pd decay (from singles measurements under collimated anti-Compton arrangement)

Transition	γ-ray energy (keV) [this work]	E_γ from scheme [a] (keV)	E_γ (keV) [ref. [7]]	Relative γ-ray intensity [this work]	Relative γ-ray intensity [ref. [7]]
2→ 1	24.4 1	24.47 5	24.46 1	20.3 8	
14→13	111.8 6	111.5 1		0.02 1	
10→ 7	129.7 10 [b]	130.1 1		0.08 4 [c]	
7→ 6	158.4 6 [b]	157.9 1		0.13 5 [c]	
6→ 5	269.66 5	269.66 5	269.60 5	30.9 10	26.8
5→ 2	296.25 5	296.23 5	296.13 2	100	100
3→ 0	305.3 6 [b]	305.3 6		≧0.19 [c]	
5→ 1	320.64 8	320.69 7	320.7 1	3.2 2	3.6
4→ 0	355.14 10	355.14 10		1.3 1	
13→ 9	380.84 25	380.93 35		0.16 4	
7→ 5	427.54 10	427.67 9		0.57 7	
14→10	435.03 25	435.15 15		0.40 6	
13→ 7	453.57 9	453.70 7	453.2 2	3.3 2	4.0
14→ 9	492.3 7	492.4 4		0.04 2	
14→ 8	496.1 6	496.3 6		0.20 8	
14→ 7	565.77 6	565.19 8	565.1 2	1.1 3 [c]	22.1
6→ 2		565.89 7		16.4 10 [c]	
6→ 1	590.36 5	590.35 6	590.3 2	61.6 10	80.1
13→ 6	611.42 20	611.66 8		0.50 10	
8→ 4	619.6 2	619.56 20		0.19 6	
11→ 4	702.6 2	702.56 20		0.08 3	
14→ 6	723.76 6	723.14 9	723.4 2	1.5 3 [c]	15.9
7→ 2		723.84 8		10.7 9 [c]	
7→ 1	748.35 8	748.29 8	748.3 6	2.6 2	3.9
15→ 7	790.2 5	790.66 12		0.13 5	
9→ 2	796.6 4	796.64 11		0.15 6	
9→ 1	821.2 6	821.10 11		0.11 6	
10→ 2	853.88 10	853.70 11		0.48 6	
13→ 5	881.32 10	881.31 8		0.62 7	
17→ 7	914.71 15	914.61 12		0.37 5	
12→ 4	965.4 3	965.26 11		0.14 8	
14→ 5	992.80 7	992.82 9	992.6 6	4.8 3	5.5
12→ 3	1014.6 3	1015.1 7		0.11 5	
16→ 6	1041.7 3	1041.59 16		0.33 5	
17→ 6	1072.6 4	1072.55 11		0.09 4	
18→ 6	1163.6 6	1163.56 16		0.05 3	
14→ 3	1165.7 6	1165.5 6		0.05 3	
13→ 2	1177.59 8	1177.63 8	1177.2 7	1.92 15	1.6

TABLE 1
(continued)

Transition	γ-ray energy (keV) [this work]	E_γ from scheme [a]) (keV)	E_γ (keV) [ref. [7])]	Relative γ-ray intensity [this work]	Relative γ-ray intensity [ref [7])]
13→ 1	1202.03 6	1201.99 8	1202.1 6	7.76 35	7.2
15→ 5	1218.27 8	1218.27 10	1218.6 8	2.8 2	2.5
14→ 2	1289.03 6	1289.04 9	1289.3 7	12.0 6	9.6
16→ 5	1311.85 9	1311.3 2	1312.8 7	1.0 2 [c])	1.5
14→ 1		1313.5 1		0.46 9 [c])	
17→ 5	1342.3 2	1342.22 11		0.11 4 [c])	
15→ 3	1391.0 6	1391.0 6		0.03 1	
18→ 5	1433.2 2	1433.23 17		0.15 4	
15→ 2	1514.5 2	1514.49 9		0.14 3	
16→ 2	1607.3 3	1607.48 16		0.12 2	
16→ 1	1632.0 3	1631.94 16		0.09 3	
17→ 2	1638.2 2	1638.44 11		0.05 1	
18→ 2	1729.3 4	1729.45 16		0.04 1	

[a]) This is the transition energy deduced from the ^{101}Rh level energies assigned in fig. 12 and given in table 5.
[b]) Energy determined from the coincidence spectra.
[c]) Intensity determined from the coincidence spectra.

TABLE 2
Energy in keV of the γ-rays contaminating the ^{101}Pd γ-ray spectra

4.5 d ^{101m}Rh	4.1 d ^{100}Pd	20 h ^{100}Rh
127	75	466
179	84	540
233	126	822 [a])
238	159	1109
307		1341
545		1362
		1555

[a]) This peak was found by decay curve analysis to have an 8.5 and a 4.1 d component associated with ^{101}Pd and ^{100}Pd–^{100}Rh decay, respectively. The ^{100}Rh fraction was for most of the cases $< 8\,\%$.

The energies of the more intense γ-rays from ^{101}Pd decay were determined by counting the ^{101}Pd samples simultaneously with standard sources of ^{57}Co, ^{139}Ce, ^{203}Hg, ^{131}I, ^{207}Bi, ^{137}Cs, ^{60}Co, ^{88}Y and ^{56}Co for internal calibration. The energies of the weaker γ-rays were determined from other spectra using the energies of the more intense γ-peaks for internal calibration. For energy calibrations a cubic equation was fit by least-squares techniques.

The relative intensities of the γ-rays were determined from full-energy peak areas using detector efficiency curves obtained by means of calibrated [16]) sources of ^{109}Cd, ^{57}Co, ^{203}Hg, ^{133}Ba, ^{180m}Hf, ^{137}Cs, ^{24}Na, ^{54}Mn, ^{60}Co, ^{88}Y and ^{56}Co.

The energies and relative intensities of γ-rays from ^{101}Pd were determined from three spectra with mixed standards and five pure ^{101}Pd spectra. The results are summarized in table 1. The first column in table 1 gives the level numbers characterizing each transition. The second and fifth columns give the γ-ray energies and

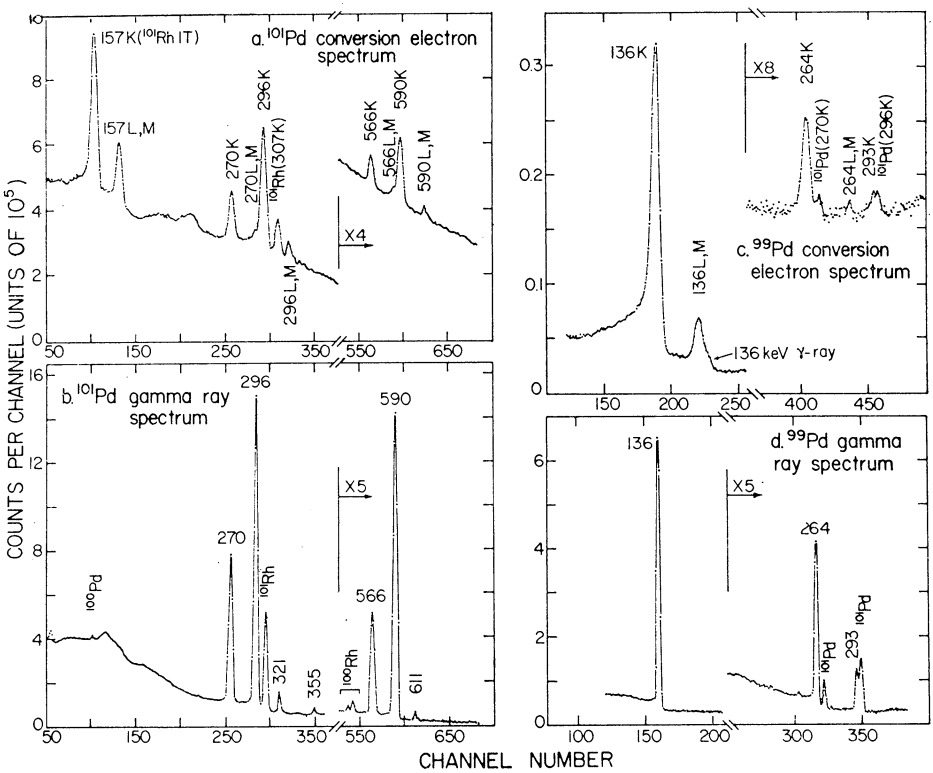

Fig. 6. Typical conversion electron spectra from ^{99,101}Pd decay are shown in the upper parts (c) and (a), respectively. These spectra were recorded with a 1 cm^2 $\times$ 1 mm Si(Li) detector in the calibrated arrangement. The lower part shows the corresponding γ-ray spectra recorded simultaneously in the Ge(Li) detector.

intensities determined in this work. The third column gives the γ-ray energies determined from the proposed decay scheme as differences between established levels, the energy of which was in turn obtained as a weighted average of the sums of the γ-ray energies leading to each level. The fourth and the last column of table 1 gives the γ-ray energies and relative intensities reported by Evans *et al.* [7])

Two additional γ-rays at 870.6 ± 0.3 and 1512.4 ± 0.2 keV with intensities 0.13 ± 0.4 and 0.16 ± 0.3 relative to the 296.25 keV taken as 100 were assigned to ^{101}Pd decay

but the present evidence does not permit definite assignment of these γ-rays in the ^{101}Pd decay scheme.

In table 2 we have summarized the energies of the γ-rays from the decay of 4.5 d ^{101m}Rh, 4.1 d ^{100}Pd and 20 h ^{100}Rh that were observed to contaminate the ^{101}Pd γ-ray spectra.

Typical spectra of the conversion electrons from sources of ^{99}Pd and ^{101}Pd are shown in the upper parts of fig. 6. The conversion electrons from the 157.32 keV isomeric transition from the growing 4.5 d ^{101}Rh are clearly seen. The lower part of figs. 6 shows the spectra of the γ-rays recorded simultaneously with the Ge(Li) detector in the calibrated geometry. Note that the 157.32 keV γ-ray from ^{101m}Rh decay is not visible in this spectrum. The K-shell conversion coefficients and the K/(L+M) ratios for some of the transitions from ^{99,101}Pd decay are summarized in table 3. The last column of table 3 gives the suggested multipolarities deduced by comparison of the experimental values with the calculated theoretical conversion coefficients [17]). The percent E2 admixture for the 136.0, 269.66 and 296.25 keV transitions was estimated from the relation $\alpha_K = [\alpha_K(M1)+\delta^2\alpha_K(E2)]/(1+\delta^2)$.

TABLE 3

Summary of the measured K-shell conversion coefficients and K/(L+M) ratios for some transitions in ^{99}Rh and ^{101}Rh following ^{99}Pd and ^{101}Pd decay

E_γ (keV)	α_K		K/(L+M)		α_{Total}		Multipolarity
transitions in ^{99}Rh							
136.0	0.165	7	6.4	4			M1+(13±4) % E2
263.6	0.0248	30					M1+(17±10) % E2
transitions in ^{101}Rh							
24.46					22.5	15	M1+(3.8±1.5) % E2 [b])
157.32 [a])	21.6	10	2.58	10	30.0	20	M4
269.66	0.022	1					M1+(10±5) % E2
296.24	0.0175	8	6.8	8	0.020	1	M1+(16±8) % E2
565.18 / 565.98	0.0035	4					M1, E2
590.35	0.0031	2					M1, E2

[a]) This is the 4.5 d isomeric transition to the ground state in ^{101}Rh.

[b]) Value calculated by comparison with α_T(M1) and α_T(E2) coefficients obtained using the theoretical threshold K-shell conversion coefficients of O'Connell and Carrol [17]) and L- and M-shell conversion coefficients of Hager and Stelson [17]).

The measurement of the internal conversion coefficients for the 24.46 and 157.32 keV transitions in ^{101}Rh together with the measurement of the percent decay by isomeric transition of the 4.5 d ^{101m}Rh deserve special mention.

Since the 157.32 keV photons were not observable in the γ-spectrum of fig. 6, pure ^{101m}Rh sources were prepared by allowing prepurified ^{101}Pd samples to decay to ^{101}Rh for a period of 24 h and then the ^{101m}Rh activity was radiochemically purified from the remaining Pd according to the procedure described in subsect. 2.1. A γ-ray and a conversion electron spectrum taken with the calibrated electron spectrometer from such a ^{101m}Rh source are shown in fig. 7. It is seen that the 157.32 keV photons are barely visible. From these experiments the ratio of 157 K-electrons to the

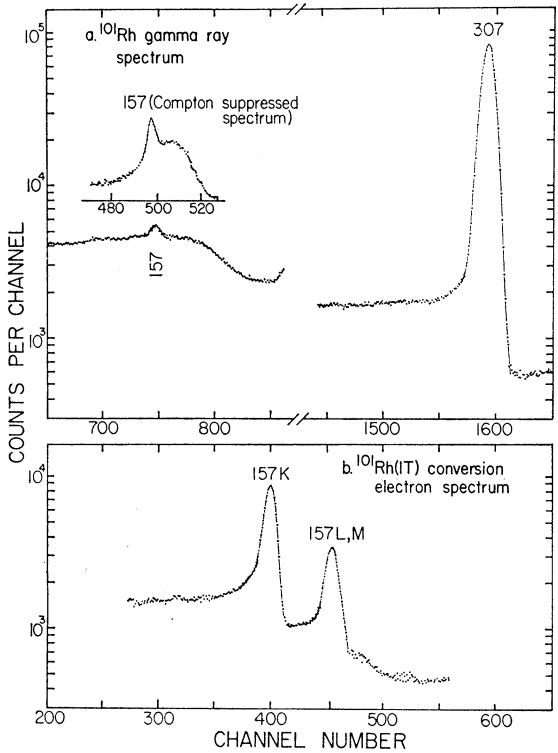

Fig. 7. The upper part (a) shows a portion of the γ-ray spectrum from a ^{101}Rh source taken with the 25 cm^3 Ge(Li) detector in the calibrated geometry. The insert shows the 157.32 keV γ-ray from a Compton suppressed spectrum. The lower part (b) shows the K and L+M conversion electrons from the isomeric transition from the same ^{101}Rh source.

^{101}Rh 307 keV photons was determined. Then the ratio of the 307 to the 157.32 keV photons from ^{101m}Rh was measured from Compton suppressed spectra (see insert in fig. 7) and was found to be 366 ± 7. This information is then used to provide (i) a more accurate value of 21.6 ± 1.0 for the K-shell conversion coefficient for the 157.32 keV isomeric transition and (ii) a value of 7.2 ± 0.5 for the percent of decays of the isomeric 157.32 keV state by isomeric transition in ^{101}Rh. This latter value is based (i) on the value of 30.0 ± 1.5 for α_{total} (157) obtained in this work; and (ii)

TABLE 4

Summary of the observed coincidence relationships of the γ-rays from ^{101}Pd decay

Fig.	Gate (keV)	γ-rays in the gate	γ-ray in coincidence (keV)
8a	254– 274 [a])	270	296, 321, 611, 723, 1042
8b	286– 304 [a])	296, 305	270, 428, 454, 565, 611, 723, 881, 993, 1015, 1042, 1218, 1311
9d	246– 298 [b])	270, 296, 305	158, 270, 296, 321, 428, 454, 565, 611, 723, 881, 915 [c]), 993, 1015, 1042, 1164, 1166, 1218, 1311, 1342, 1391, 1433
8c	304– 322 [a])	305, 321	270, 723, 993, 1015
8d	322– 340 [a])	321	270, 723, 993
9c	340– 390 [b])	355, 381	496, 620, 703, 797, 821, 965
10a	423– 439 [a])	428, 435	130, 296, 454, 565, 854
	400– 450 [b])	428, 435, 454	112, 130, 296, 321, 428, 454, 565, 724, 748, 790, 854, 915
10b	439– 457 [a])	454	158, 428, 724, 748
11b	558–575 [a])	565, 566	158, 611, 723, 724, 748
11c	575– 593 [a])	590	158, 611, 723
9b	545–600 [b])	565, 566, 590, 611	158, 270, 296, 355, 428, 496, 566, 590, 611, 723, 724, 748 [c]), 1042, 1073, 1164
11e	716– 734 [a])	723, 724	270, 296, 321 [c]), 454, 565, 566, 590, 790
11f	734– 752 [a])	748	454, 565
9a	706– 758 [b])	703, 723, 724, 748	112, 130, 270, 296, 321, 355 [c]) 435 [c]), 454, 565, 566, 590, 790, 915
	760– 810 [b])	790, 797, 821	296, 381, 492 [c]), 724, 854 [c]), 871
	810– 865 [b])	797, 821, 854, 871	381, 435, 492, 854 [c]), 871
	865– 915 [b])	854, 871, 881, 915	296, 321, 435, 724, 748
	915– 967 [b])	915, 965	355, 724, 748
	982–1000 [a])	993	296, 321
	967–1010 [b])	965, 993, 1015	296, 305, 321, 355, 724
	1125–1175 [b])	1164, 1166, 1178	112, 270, 296, 566, 590
	1175–1235 [b])	1178, 1202, 1218	112, 296, 321
	1285–1335 [b])	1289, 1311, 1314, 1342	296, 321
	1335–1390 [b])	1342, 1391	296, 305, 321
	1390–1450 [b])	1391, 1433	296, 305, 321

[a]) From Ge(Li)–Ge(Li) coincidence experiments.
[b]) From NaI(Tl)–Ge(Li) coincidence experiments.
[c]) Weak coincidence.

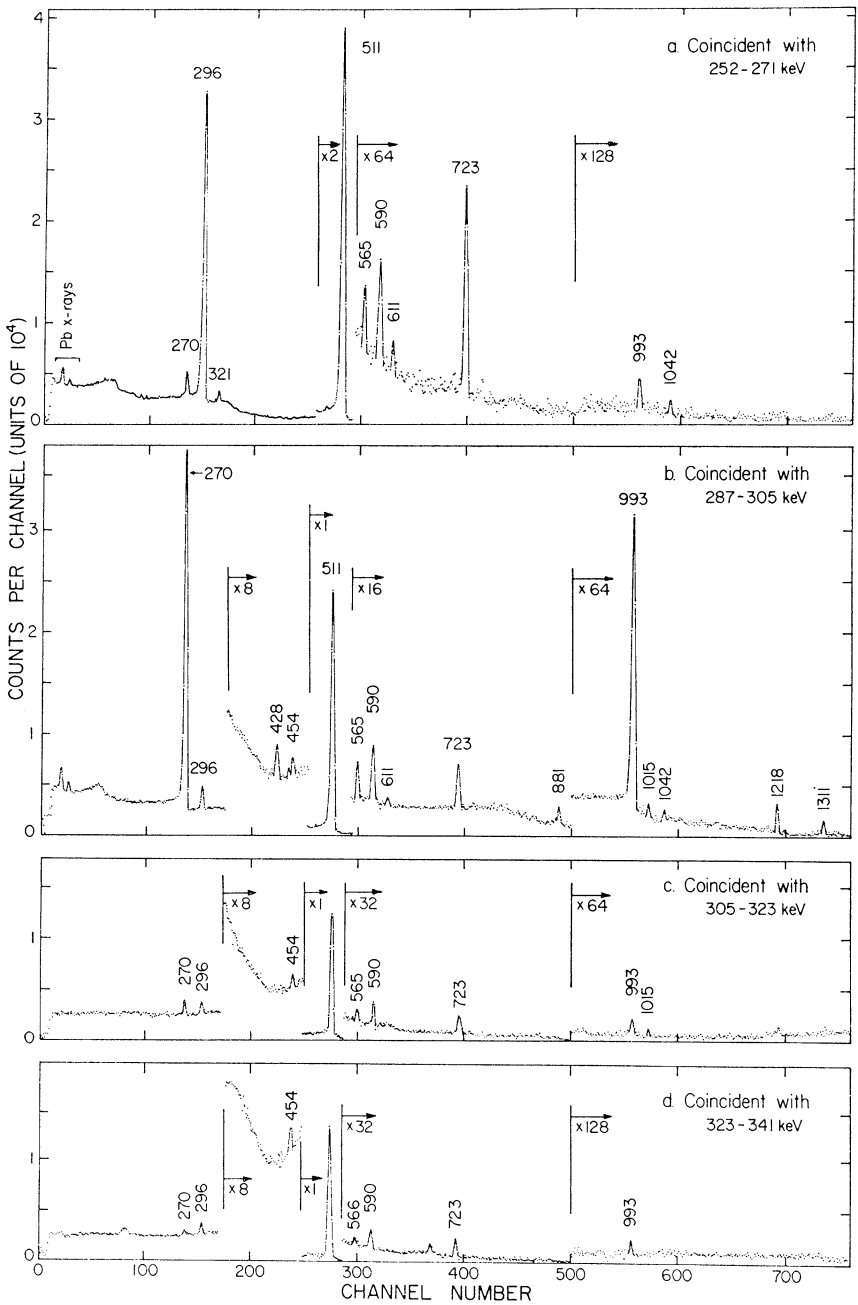

Fig. 8. Spectra of the γ-rays from ^{101}Pd decay observed with the 25 cm^3 Ge(Li) detector in coincidence with the indicated energy regions in the 29 cm^3 Ge(Li) detector. Gate (a) includes the 269.66 keV γ-ray, gate (b) the 296.25 and part of the 305.3 keV γ-rays, gate (c) part of the 305.3 and 320.64 keV γ-rays and gate (d) part of the 320.64 keV γ-ray and the underlying Compton background.

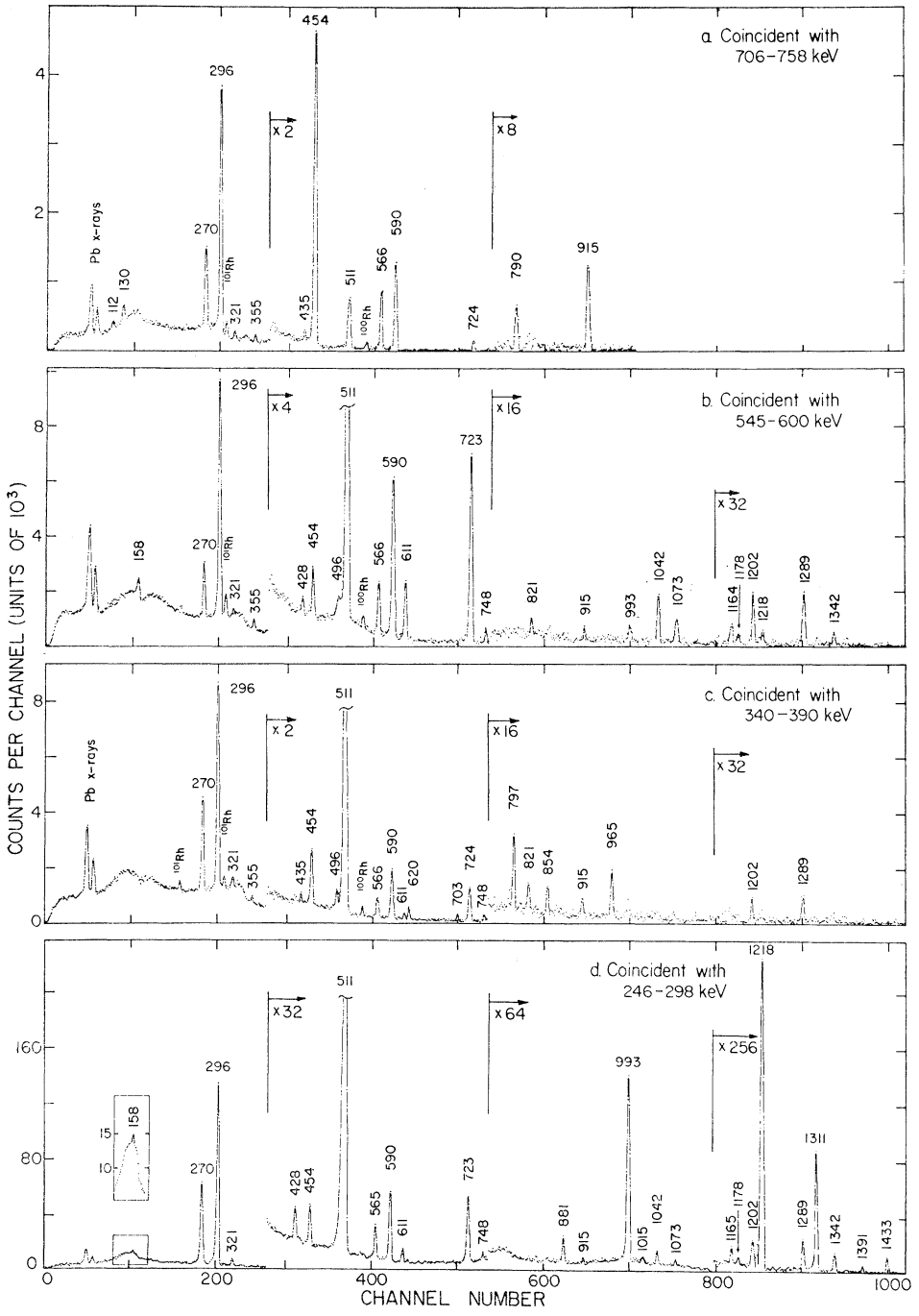

Fig. 9. Spectra of the γ-rays from ^{101}Pd decay observed with the 25 cm^3 Ge(Li) detector under Compton suppression in coincidence with the indicated regions in the NaI(Tl) detector. The γ-rays included in the NaI(Tl) gates are listed in table 4.

on the value of 93.5 given by Evans and Naumann [18]) for the percentage of decays in ^{101}Ru through the 307 keV γ-ray following 4.5 d ^{101m}Rh decay. Our value for the percent of isomeric transition disagrees with the value of 10 % given by Evans *et al.* [7]). Using the K and L+M relative intensities for the conversion electrons for IT in ^{101}Rh and the 307 keV transition in ^{101}Ru given by Evans *et al.* [7]) and our α_T (157) value of 30.0±1.5 we calculate 7.21 for the percent of IT in ^{101}Rh, in excellent agreement with our independent measurements.

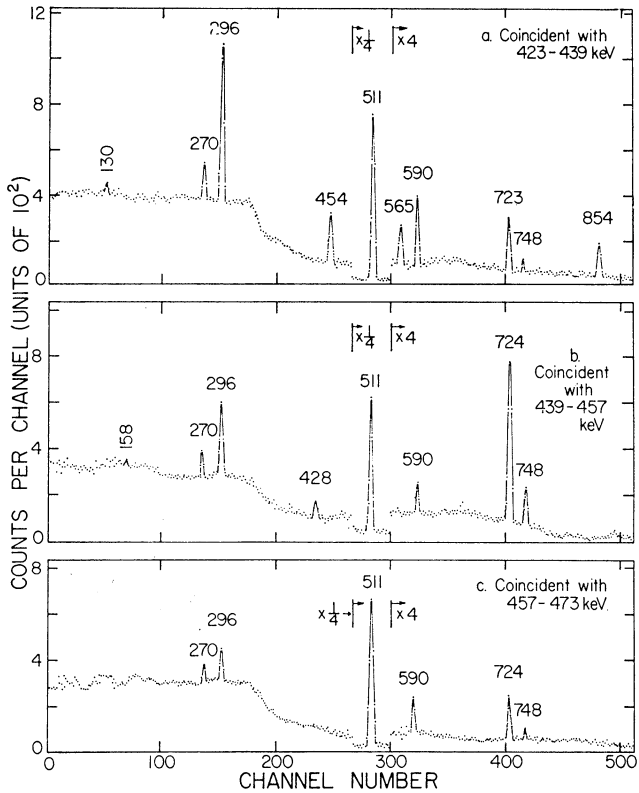

Fig. 10. Spectra of the γ-rays from ^{101}Pd decay observed with the 25 cm^3 Ge (Li) detector in coincidence with the indicated energy regions in the 29 cm^3 Ge(Li) detector. Gate (a) includes the 427.54 and 435.03 keV γ-rays, gate (b) the 453.57 keV γ-ray and gate (c) the Compton background.

The total conversion coefficient for the 24.46 keV transition in ^{101}Rh was obtained from (i) the measured photon intensity of 20.3±0.8 for the 24.46 keV transition relative to the 296.25 keV taken as 100, and (ii) the total γ-ray intensity of 468±18 obtained on the basis of the proposed decay scheme. It is important to note that the result of $\alpha_T = 22.5 \pm 1.5$ is consistent with primarily an M1 assignment for the 24.46 keV transition as the theoretical values [17]) are $\alpha_T(M1) = 14.9$, $\alpha_T(E1) = 6.1$ and $\alpha_T(E2) = 224.0$. The threshold values of O'Connell and Carrol [17]) for the K-shell

conversion of the 24.46 keV transition were used for the theoretical $\alpha_K(M1)$ and $\alpha_K(E2)$ coefficients. For the L- and M-shell conversion the α_L, α_M values of Hager and Seltzer [17]) were used. The M1 assignment is also in agreement with the findings of Evans *et al.* [7]) who assigned this transition as M1 on the basis of $L_I/L_{II}/L_{III}$ ratios.

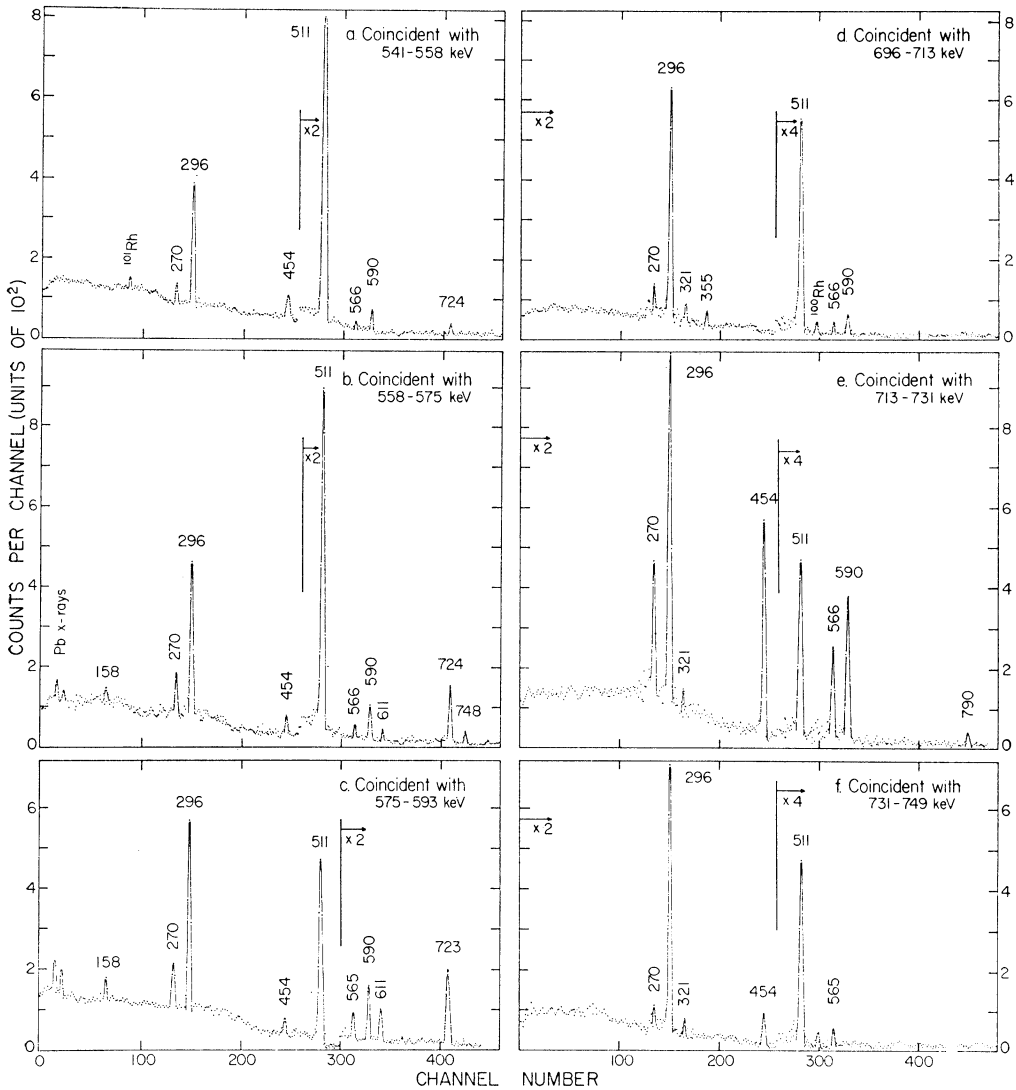

Fig. 11. Spectra of the γ-rays from ^{101}Pd decay recorded with the 25 cm^3 Ge(Li) detector in coincidence with the indicated regions in the 29 cm^3 Ge(Li) detector. Gate (a) contains only Compton background, gate (b) contains the 565.2 and 565.9 keV γ-rays, gate (c) the 590.36 keV γ-ray, gate (d) the 702.6 keV γ-ray, gate (e) the 723.14 and 723.84 keV γ-rays and gate (f) the 748.35 keV γ-ray.

The $\gamma\gamma$ coincidence relationships were established in this work on the basis of Ge(Li) × Ge(Li) and NaI(Tl) × Ge(Li) two parameter experiments in a 256 × 1024 channel configuration. The coincidence relationships are summarized in table 4 and representative spectra are shown in figs. 8-11. Although the Na(Tl) × Ge(Li) coincidence spectra suffer from poor resolution in the gating NaI(Tl) axis, they are of good statistical quality and help establish many coincidence relationships which involve the weaker higher energy γ-rays.

Due to the complexity of the ^{101}Pd decay scheme and the evidence from $\gamma\gamma$ coincidence experiments for seven unresolved doublets (see fig. 4) it was considered necessary to perform a triple coincidence experiment. In this experiment the ^{101}Pd source was wrapped with sufficient Cu foil to completely absorb the Rh X-rays and the 24.46 keV γ-ray. The following γ-rays were observed to participate in triplet $\gamma\gamma\gamma$ coincidences: 111.8, 158.4, 269.66, 296.25, 320.64, 355.14, 427.54, 453.57, 496.1, 565.2, 611.42, 619.6, 723.2, 1041.7 and 1072.6 keV.

Finally, we mention that Evans *et al.* [7]) have reported the 296.25, 565.9, 723.8, 881.32, 1177.6, 1218.27 and 1289.03 keV γ-rays in coincidence with the L-conversion electrons of the 24.46 keV transition. Furthermore from their data it is seen that the 853.88 keV γ-ray is also in coincidence with the L-electrons of the 24.46 keV transition.

4. Construction of the decay scheme and assignment of J^π values

From the evidence presented above we propose the decay scheme shown in fig. 12. In table 5 we have summarized the proposed level energies, the percent ($\beta^+ + $EC) and EC populations, the determined log ft values, and the assigned J^π value to each

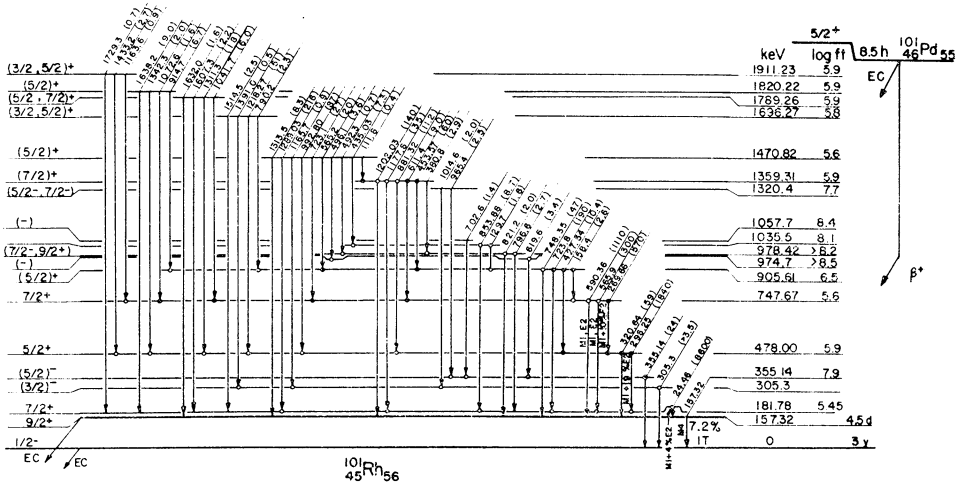

Fig. 12. Proposed decay scheme for 8.5 h ^{101}Pd. The energies are given in keV and the transition intensities in parentheses are given per 10^4 decays.

proposed level. The percent ($\beta^+ + EC$) population was determined by difference of the total transition intensity depopulating and populating each level. The percent population by EC of each level was obtained using the β^+/EC ratios given in p. 575 of ref. [19]). The log ft values reported in the fifth column of table 5 were obtained using the nomograms in pp. 573 and 574 of ref. [19]). Below we summarize the arguments supporting the proposed decay scheme and the J^π assignments.

TABLE 5
Assignment of log ft and J^π values to levels ^{101}Rh

Level no.	Level energy (keV)		%(β^++EC)		%EC		log ft		J^π
0									$\frac{1}{2}^-$
1	157.32	3							$\frac{9}{2}^+$
2	181.78	3	59.9	18	53.0	18	5.45	10	$\frac{7}{2}^+$
3	305.3	6							$\frac{3}{2}^-$, $(\frac{5}{2})^-$
4	355.14	10	0.16	3	0.15	3	7.9	1	$\frac{5}{2}^-$, $(\frac{3}{2})^-$
5	478.00	5	11.5	4	11.2	4	5.9	1	$\frac{5}{2}^+$
6	747.67	4	19.4	3	19.4	3	5.6	1	$\frac{7}{2}^+$
7	905.61	7	1.62	18	1.62	18	6.5	1	$(\frac{5}{2})^+$
8	974.7	2	−0.002	18	<0.016		>8.5		(−)
9	978.42	10	0.011	18	0.011	18	>8.2		$(\frac{7}{2}^-, \frac{9}{2}^+)$
10	1035.5	1	0.031	16	0.031	16	8.1	3	
11	1057.7	2	0.014	5	0.014	5	8.4	2	(−)
12	1320.4	3	0.045	16	0.045	16	7.7	2	$(\frac{5}{2}^-, \frac{7}{2}^-)$
13	1359.31	7	2.57	8	2.57	8	5.9	1	$(\frac{7}{2})^+$
14	1470.82	8	3.71	15	3.71	15	5.6	1	$(\frac{5}{2}^+)$
15	1696.27	9	0.56	4	0.56	4	5.8	1	$(\frac{3}{2}, \frac{5}{2})^+$
16	1789.26	15	0.28	5	0.28	5	5.9	1	$(\frac{5}{2}, \frac{7}{2})^+$
17	1820.22	10	0.19	2	0.19	2	5.9	1	$(\frac{5}{2})^+$
18	1911.23	15	0.043	9	0.043	9	5.9	1	$(\frac{3}{2}, \frac{5}{2})^+$

The ground state of ^{101}Pd can be assumed as $\frac{5}{2}^+$ on two grounds: (i) all the odd-mass Pd isotopes from A = 103–109 have been assigned as $\frac{5}{2}^+$ from the (d, p) and (d, t) work of Cujec [20]) and by analogy ^{101}Pd is also $\frac{5}{2}^+$ and (ii) from the decay of 21 min ^{99}Pd it was found [8]) that the $\frac{9}{2}^+$ metastable state in ^{99}Rh is not populated by the beta decay processes thus limiting the ^{99}Pd ground state as $\frac{5}{2}^+$. This evidence makes very unlikely any assignment other than $\frac{5}{2}^+$ for the ^{101}Pd ground state.

The ground state and the 157.32 keV 4.5 d *metastable state.* Arguments for the assignment of the ground state of ^{101}Rh has $\frac{1}{2}^-$ and the metastable state as $\frac{9}{2}^+$ based on K/(L+M) ratios have been presented by Evans *et al* [7]). In this work we have measured the α_K for the isomeric transition in ^{101}Rh and found it to be 21.6±1.0 in excellent agreement with the theoretical value [17]) of 21.7 for the M4 transition. Since

the 4.5 d isomeric state decays to populate the $(\frac{7}{2})^+$ 306.7 keV state in ^{101}Ru by an allowed transition it is assigned as $\frac{9}{2}^+$ in agreement with the findings of Evans *et al.* [7]). Furthermore, the ^{103}Rh ground state has been measured [21]) to be $\frac{1}{2}$ and from systematics its parity is negative. Level systematics in the odd-mass Rh isotopes indicate that the ^{101}Rh ground state should also be $\frac{1}{2}^-$. The J^π assignments of $\frac{1}{2}^-$ and $\frac{9}{2}^+$ for the ground and metastable state in ^{101}Rh, are therefore, consistent with the evidence given above.

The 181.78 keV *level.* Seven pairs of γ-rays differing in energy by approximately 24.4 keV were observed to follow ^{101}Pd decay and one γ-ray in each of five of these pairs was observed in coincidence with the L-conversion electrons from the 24.46 keV transition [7]). This information together with the fact that the 24.46 keV transition is the most intense one require it to populate directly the ground or the metastable state. From the $L_I/L_{II}/L_{III}$ ratio work of Evans *et al.* [7]) the 24.46 keV transition is M1. This assignment is also substantiated by our measurement of 22.5 ± 1.5 for the total conversion coefficient for the 24.46 keV transition when compared to the values [17]) of 6.1, 14.9 and 224 for E1, M1 and E2, respectively. The strong positon group with an end-point energy of 785 ± 15 keV observed by Evans *et al.* [7]) to follow ^{101}Pd decay may be accommodated to populate the 181.78 keV level and not the $\frac{9}{2}^+$ isomeric state at 157.32 keV.

Furthermore, from a study of the ^{100}Ru(^{3}He, d)^{101}Rh reaction [22]) we find evidence for levels at 157 and 182 keV in ^{101}Rh but not at 24 keV. This result and the γ-ray information definitely establish the level at 181.78 keV. Since the 24.46 keV transition is M1 and the 181.78 keV level is strongly populated by EC from the $\frac{5}{2}^+$ ^{101}Pd decay its J^π value can be limited to only $\frac{7}{2}^+$.

The 305.3 keV *level.* The direct observation of a γ-ray at this energy that de-excites this level to the ground state is masked by the presence of a strong γ-ray at that energy from the daughter ^{101}Rh. A level at 305 keV, however, was observed in the ^{100}Ru(^{3}He, d) reaction [22]) and the 305.3 keV γ-ray was observed in coincidence with γ-rays at 1014.6, 1165.7 and 1391.0 keV (fig. 8b and table 4). These coincident γ-rays connect with well established levels at 1470.82 and 1696.27 keV (see fig. 12 and discussion below) and help establish another level at 1320.4 keV. The intensity of the 305.3 keV γ-ray is too low to allow a direct determination and a lower limit is given in table 1 based on the sum of the intensities of the γ-rays populating this level. The fact that the 305.3 keV level does not appear to be populated by beta decay and it decays only to the $\frac{1}{2}^-$ ground state, strongly suggests a negative parity and J^π of ($\frac{3}{2}^-$ or $\frac{5}{2}^-$) for this level.

The 355.14 keV *level.* A level at this energy in ^{101}Rh was observed in the ^{100}Ru(^{3}He, d) reaction [22]). This level is believed to be populated also in the decay of ^{101}Pd on the basis of the observed coincidences of the 355.14 keV γ-ray with the 496.1, 619.6, 702.6 and 965.4 keV γ-rays (fig. 9c). The 355.14 keV γ-ray was not observed in coincidence with any of the intense γ-rays. Furthermore the three γ-rays at 355.14, 619.5 and 496.1 keV have an energy sum of 1470.84 keV in excellent

agreement with the well-established level at this energy (see fig. 12). Since the 355.14 keV γ-ray has an intensity exceeding the sum of the intensities of the γ-rays with which it is in coincidence, it was assigned to populate the ground state.

The log ft value of 7.9 for the population of this level suggests a probable first forbidden transition. This and the fact that this level decays only to the $\frac{1}{2}^-$ ground state support a most probable assignment of $\frac{3}{2}^-$ or $\frac{5}{2}^-$ for the 355.14 keV level. By comparison with the $\frac{3}{2}^-$ and $\frac{5}{2}^-$ states in ^{103,105}Rh (see fig. 13a) it is seen that the 355.14 keV level in ^{101}Rh is most likely $\frac{5}{2}^-$ while the 305.3 keV level is most likely $\frac{3}{2}^-$.

The 478.00 keV *level.* This level is well established on the basis of the following evidence: (i) the observed coincidence of the 296.25 keV γ-ray with the L-conversion

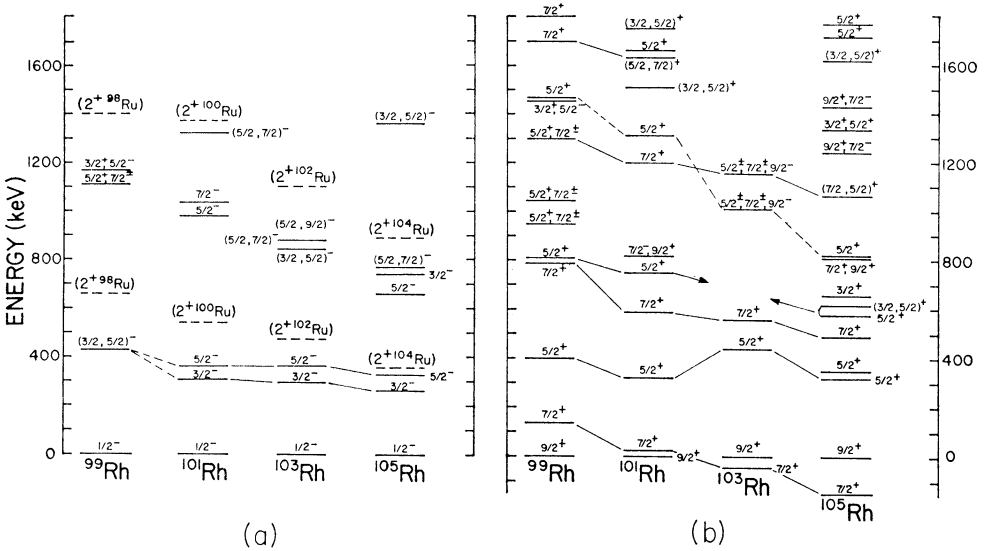

Fig. 13. Part (a) shows the trend of the negative parity states in $^{99-105}$Rh with neutron number. The first and second 2^+ states of the even cores are also shown by dashed lines. Part (b) summarizes the available experimental information for the positive parity states in $^{99-105}$Rh. The level energies are presented relative to the $\frac{9}{2}^+$ state. Levels believed to be of similar nature are joined by lines.

electrons of the 24.46 keV transition, (ii) the observed crossover 320.64 keV transition to the 157.32 keV metastable state, and (iii) the wealth of γ-rays observed in coincidence with both the 296.25 and 320.64 keV γ-rays (see figs. 8b, c, 9d, 12 and table 4).

This 478.00 keV level is strongly populated by (EC+β^+) decay (log ft = 5.9) and decays to the $\frac{7}{2}^+$ 181.78 keV state and to the $\frac{9}{2}^+$ 157.32 keV metastable state with a branching ratio of 31.4 : 1.0. This strong 296.25 keV transition is primarily M1 (see table 3). This evidence strongly suggests a $\frac{5}{2}^+$ assignment for this level.

The 747.67 keV *level.* This level is firmly established on the basis of the strong coincidence of the 269.66 keV γ-ray with the 296.25 and 320.64 keV γ-rays (figs.

8a, b). The 590.36 keV γ-ray is assigned as the stopover transition to the metastable state. It is important to note here that the peaks at 566 and 723 keV are shown to be unresolved doublets on the basis of the following evidence. The 723 keV peak is seen in coincidence with the 566 keV peak (figs. 11b, e). The 723 keV peak is also seen in coincidence with the 269.66 and 590.36 keV γ-rays (figs. 8a, 11c). The 723 keV peak is further observed in coincidence with the 453.57, 790.2 and 914.7 keV γ-rays (fig. 9a). This is sufficient evidence to place a 723.1 keV γ-ray to de-excite a well established level at 1470.82 keV and a 723.8 keV γ-ray to de-excite another well established level at 905.61 keV. This is further substantiated by the observation of the 723.1 keV γ-ray in triple coincidence with γ-rays (not including the 24.46 keV γ-ray). The intensity of the 723.1 keV γ-ray that de-excites the 1470.82 keV level was obtained from the peak areas of the 611.4 and 723.1 keV γ-rays in the Ge(Li) $\times$ Ge(Li) coincidence spectra (figs. 8a, b and 11c).

The 566–724 coincidence can be accommodated by either of the following two cascades (i) 1470.82 $\rightarrow$ 905.61 $\rightarrow$ 181.78 keV and (ii) 1470.82 $\rightarrow$ 747.67 $\rightarrow$ 181.78 keV. Evidence for the former cascade comes from the observed coincidence of the 565.2 keV γ-ray with the 427.54 and 748.35 keV γ-rays (figs. 10a, 11f). Evidence for the latter cascade comes from the observed coincidence of the 565.9 keV γ-ray with the 158.4, 611.4, 1041.7, 1072.6 and 1163.6 keV γ-rays (figs. 11b, 9b). The observation of the 158.4, 611.4, 1041.7 and 1072.6 keV γ-rays in the triple coincidence spectrum further substantiates the above assignments.

The intense decay of this 747.67 keV level to the $\frac{9}{2}^+$ metastable state and the weaker decay to the $\frac{7}{2}^+$ state at 181.78 by M1 or E2 transitions (table 3) strongly supports a $\frac{7}{2}^+$ assignment. This also is supported by the allowed character of the (EC+β^+) decay to this level (log ft = 5.6) and the observed M1 character of the 269.66 keV transition (table 3) to the $\frac{5}{2}^+$ 478.00 keV level below.

The levels at 905.61 *and* 1470.82 keV. Both of these levels are firmly established from many coincidences as shown in fig. 12. Thus four γ-rays were assigned to de-excite the 905.61 keV level and ten γ-rays were assigned to de-excite the 1470.82 keV level. Both of these levels are strongly populated by electron capture decay (log ft values 6.5 and 5.6). These two levels populate strongly $\frac{5}{2}^+$ and $\frac{7}{2}^+$ levels below and only rather weakly the $\frac{9}{2}^+$ metastable state. This evidence makes most probable a $\frac{5}{2}^+$ assignment for the 905.61 keV level. The 1470.82 keV level is also assigned as $\frac{5}{2}^+$, since in addition to the $\frac{5}{2}^+$ and $\frac{7}{2}^+$ states to which it decays strongly, it was observed to populate the $\frac{3}{2}^-$ state at 305.3 keV.

The 978.42 keV *level.* This level is established on the basis of two γ-rays at 796.6 and 821.4 keV, with an energy difference of 24.8$\pm$0.7 keV, observed in coincidence with the 380.8 keV γ-ray (fig. 9c) which has been assigned to de-excite the well established level at 1359.31 keV (fig. 12). These two γ-rays at 796.6 and 821.2 keV also appear to be in coincidence with the 492.3 keV γ-ray (table 4) which de-excites the well established level at 1470.82 keV. A level at this energy was also observed [22]) in the ^{100}Ru(^{3}He, d)^{101}Rh reaction. This 978.42 keV level does not appear to be populated

by EC decay ($\log ft > 8.2$) and it is only populated by a very weak branch from the $\frac{5}{2}^+$ level at 1470.82. This information and the fact that it decays exclusively to the $\frac{9}{2}^+$ and $\frac{7}{2}^+$ levels at 157.32 and 181.78 keV suggest that its J^π value is not likely to be $\frac{3}{2}^+$, $\frac{5}{2}^+$ or $\frac{7}{2}^+$. If the parity of this level were negative then its J^π value would be limited to $\frac{7}{2}^-$ only. If this level were $\frac{7}{2}^-$ then the decay to the $(\frac{3}{2}, \frac{5}{2})^-$ levels at 305.3 and 355.15 keV should have been observed. An upper limit for these transitions can be placed at 0.8 per 10^4 decays. A value of $\frac{9}{2}^+$ for this level is quite probable from the present evidence.

A level at 974.7 keV. The two γ-rays at 619.6 and 496.1 keV have been observed in strong coincidence with each other (fig. 9b) and with 355.14 keV γ-ray (fig. 9c). The energy sum $355.14+619.6+496.1 = 1470.84 \pm 0.60$ keV is in excellent agreement with the level at this energy. These three γ-rays have been observed in the triple coincidence spectrum. The intensities of the 496.1 and 619.6 keV γ-rays are equal within experimental error. Placing the 496.1 keV γ-ray to populate the 355.14 keV level would require a level at 851.0 keV. No such level was observed in the ^{100}Ru(^{3}He, d) reaction [22]). However, placing the 619.6 keV γ-ray to populate the 355.14 keV level would require a new level at 974.74 keV, which is too close to be resolved from the 978.42 keV level in the ^{100}Ru(^{3}He, d) reaction [22]) which shows a level at 976 keV. We prefer this assignment over that for an 851.0 keV level and note that the parity for this 974.74 keV level is most likely negative since it decays exclusively to the $(\frac{5}{2})^-$ level at 355.14 keV and it is not populated by electron capture.

The 1035.5 keV *level.* A new level at this energy is established on the basis of the observed coincidence of the 129.7 keV γ-ray with the 427.54, 723.8, 748.35 and 435.03 keV γ-rays (figs. 9a, 10a). The 129.7 keV γ-ray thus populates the 905.61 keV level. This new level is further supported by the observed coincidence of the 853.88 γ-ray with the 435.03 keV γ-ray (see table 4) and the fact that the sum $853.88+435.03$ keV is equal to the energy difference of the 1470.82 and 181.78 keV levels. Furthermore, from the work of Evans *et al.* [7]) it appears that the 853.88 keV γ-ray is in coincidence with the L-conversion electrons from the 24.46 keV transition.

The present evidence is insufficient for a J^π assignment.

The 1320.4 keV *level.* The two weak γ-rays at 965.4 and 1014.6 keV have been observed in coincidence only with the 355.14 and 305.3 keV γ-rays, respectively (figs. 9c, 8b), and have been assigned to de-excite a new level at 1320.4 keV. This information together with the large $\log ft$ value of 7.7 for this level and the lack of decay to the $\frac{1}{2}^-$ ground state suggest a probable $\frac{5}{2}^-$ or $\frac{7}{2}^-$ assignment for this level.

The 1359.31 keV *level.* This level is firmly established on the basis of observed coincidences of five γ-rays that have been assigned to de-excite it with other γ-rays de-exciting established levels below (fig. 12). The strong population of this level by electron capture ($\log ft = 5.9$) and its intense decay to the $\frac{9}{2}^+$ 157.32 keV level support a $\frac{7}{2}^+$ assignment for this level.

The 1696.27 *and* 1911.23 keV *levels.* The γ-rays at 790.2, 1218.27 and 1391.0 keV have been observed in coincidence with the 723.8, 296.25 and 305.3 keV γ-rays,

respectively (figs. 9a, 8b and 9d). This information firmly establishes the level at 1696.27 keV. The presence of this level was also suggested by Evans *et al.* [7]).

The γ-rays at 1163.6 and 1433.2 keV were seen in coincidence with the 590.36 and 296.25 keV γ-rays, respectively (figs. 9b, d). This establishes a new level at 1911.23 with the 1729.3 keV γ-ray assigned as crossover to the 181.78 keV level. Both of these levels are strongly populated by electron capture ($\log ft = 5.9$) and are observed to decay to $\frac{5}{2}^+$ and $\frac{7}{2}^+$ levels below but not to the $\frac{9}{2}^+$ 157.32 keV level. This information is sufficient to limit the J^π value for both of these levels to $\frac{3}{2}^+$ or $\frac{5}{2}^+$.

The 1789.26 keV *level.* This new level is established on the basis of the observed coincidence of the 1041.7 and 1311.3 keV γ-rays with the 590.36 and 296.25 keV γ-rays, respectively (figs. 9b and 9d). The 1607.3 and 1632.0 keV γ-rays were assigned as crossover transitions populating the 181.78 and 157.32 keV levels on the basis of good energy agreement. This level is populated via electron capture by an allowed transition ($\log ft = 5.9$) and it further decays strongly to the $\frac{9}{2}^+$ 157.32 and $\frac{7}{2}^+$ 181.78 keV levels. This evidence limits the J^π value for this level to $\frac{5}{2}^+$ or $\frac{7}{2}^+$ with the $\frac{7}{2}^+$ being the most probable one.

The 1820.22 keV *level.* This new level is established by the observed coincidences of the 914.7, 1072.6 and 1342.3 keV γ-rays with the 748.35, 590.36 and 296.25 keV γ-rays, respectively (figs. 9a, b and d). By good energy agreement the 1638.2 keV γ-ray was assigned as crossover to the 181.78 keV level. The allowed character of the electron capture decay to this level ($\log ft = 5.9$), its strong decay to $\frac{5}{2}^+$ and $\frac{7}{2}^+$ levels below and the lack of decay to the $\frac{9}{2}^+$ state below, limit the J^π value for this level to $\frac{3}{2}^+$ or $\frac{5}{2}^+$. The rather strong population of the $\frac{7}{2}^+$ 181.78 keV state favors the $\frac{5}{2}^+$ assignment as the most probable one.

A possible level at 1057.7 keV. A level at this energy is indicated by the observed coincidence of the 702.6 keV γ-ray with the 355.14 keV γ-ray (fig. 9c). No other γ-ray that could de-excite or populate this level was observed. A level at 1047 ± 8 was observed [22]) in the ^{100}Ru(^{3}He, d) reaction and it could originate from an unresolved 1035.5 and 1057.7 keV doublet.

5. Discussion and interpretation of levels

The decay scheme proposed in this work is found in excellent agreement with the simpler scheme proposed by Evans *et al.* [7]) and in addition to the levels at 157.32, 181.78, 478.00, 474.67, 905.61, 1359.31 and 1470.82 keV reported by Evans *et al.* [7]) new levels in ^{101}Rh at 305.3, 355.14, 974.7, 978.42, 1035.5, 1057.7, 1320.4, 1696.27, 1789.26, 1820.22 and 1911.23 keV have been found to be populated in the decay of 8.5 h ^{101}Pd. Additional evidence for the presence of levels at these energies in ^{101}Rh was also obtained [22]) from the ^{100}Ru(^{3}He, d) reaction. The proposed decay scheme is found in serious disagreement with that put forth by Dzhelepov *et al.* [6]) and with the exception of the 157.32 keV metastable state and the 201, 500 and 922 keV levels which have been displaced by 19 keV to higher energies we find no evidence

for levels at 790, 1200, 1355, 1526, 1640 or 1672 keV. We have further attempted to identify the reported transition energies with the hope to use their relative electron intensities to calculate conversion coefficients, but we find meaningless values for the K-shell coefficients of the high-energy γ-rays.

In the discussion of the nature of the states in the odd-mass Rh isotopes it is instructive to distinguish the positive from the negative parity states. In this case, the negative parity states (e.g. the $\frac{1}{2}^-$ ground state) may arise from particle-hole configurations of the type $[p_{\frac{1}{2}}^{-1}(g_{\frac{9}{2}})^6]$. Other particle-hole configurations with holes in the $2p_{\frac{3}{2}}$ and $1f_{\frac{5}{2}}$ subshells will give rise to single-particle states at higher energy.

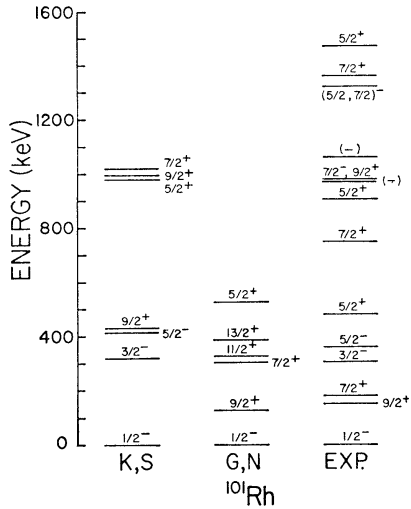

Fig. 14. Comparison of the experimental level structure of ^{101}Rh with the results of the EQPC theory [12]) indicated by G, N and with the results of the QPC theory [9]) indicated by K, S.

On the other hand, the first low-lying negative parity states $\frac{3}{2}^-$ and $\frac{5}{2}^-$ can be described to first order in terms of either the $p_{\frac{3}{2}}$ single-particle ground state coupled to the 2^+ state of the core as suggested by de-Shalit [23]), and Lawson and Uretzky [24]), or in terms of the quasiparticle-phonon coupling model (QPC) of Kisslinger and Sorensen [9]). In the limit of the weak coupling model [23]) the center of gravity theorem [24]) for "spherical" nuclei indicates that the splitting of the $\frac{3}{2}^-$ and $\frac{5}{2}^-$ doublet should be small and its center of gravity equal to the energy of the 2^+ state of the doubly even core. Experimentally, the $\frac{3}{2}^-$, $\frac{5}{2}^-$ splitting is small, but the c.m. theorem is violated. In fig. 13a we have summarized the presently available experimental information on the negative parity states in $^{99-105}Rh$. The $\frac{3}{2}^-$ and $\frac{5}{2}^-$ doublet is clearly and systematically seen to lie lower than the 2^+ state of the underlying core, presumably due to pairing interactions. This seems to be the case in all the odd-mass Tc, Rh and Ag isotopes [19]). These two levels are also predicted reasonably well by the QPC calculations of Kisslinger and Sorensen [9]) as is shown in fig. 14.

Black *et al.* [25]) have measured the $B(E2)$ values for the $\frac{3}{2}^- \rightarrow \frac{1}{2}^-$ and $\frac{5}{2}^- \rightarrow \frac{1}{2}^-$ transitions in ^{103}Rh and for the $2^+ \rightarrow 0^+$ transitions in the neighboring doubly even nuclei ^{102}Ru and ^{104}Pd and found all these to be equal within experimental error. This result together with the observation that $B(E2)_{exp}/B(E2)_{s.p.} \approx 40$ for these transitions is indicative of a collective nature of these states. Black *et al.* [25]) have also calculated the $B(M1)_{exp}/B(M1)_{s.p.}$ ratio for the transitions from the $\frac{3}{2}^-$ 295 keV state to the $\frac{1}{2}^-$ ground state and from the $\frac{5}{2}^-$ 357 keV state to the $\frac{3}{2}^-$ 295 keV state in ^{103}Rh and found them to be ≈ 0.22 and ≈ 0.21, respectively. Since M1 transitions from members of the phonon coupled multiplet to single quasiparticle levels are forbidden and M1 transitions between members of the multiplet are allowed (but hindered) these ratios could be explained within the framework of these models, by small single-particle admixtures. The qualitative form of these models is substantiated by the similar (p, p') angular distributions for the $\frac{3}{2}^-$ and $\frac{5}{2}^-$ states observed [25]) in ^{103}Rh and for the 2^+ state in the neighboring doubly even nuclei.

Black *et al.* [25]) have interpreted the four negative parity states at 789, 843, 877 and 915 keV in ^{103}Rh as arising primarily from the coupling of the $p_{\frac{1}{2}}$ state to the 2^+ and 4^+ two-phonon states of the core. We believe that although these states may have considerable two-phonon $p_{\frac{1}{2}}$ character other single quasiparticles and phonon coupled $p_{\frac{3}{2}}^{-1}$ and $f_{\frac{5}{2}}^{-1}$ quasiparticle states may contribute to a significant extent. Black *et al.* [25]) have also observed that in ^{103}Rh these four higher energy negative parity states appear to decay almost exclusively to the $(\frac{3}{2}^-)$ 295 keV and $(\frac{5}{2}^-)$ 358 keV doublet. A similar tendency may exist in the de-excitation of the analogous levels in ^{101}Rh. Thus, the 974.7, 1057.7 and 1320.4 keV levels have been seen to decay only to the 305.3 and 355.14 keV doublet. However, their weak population in ^{101}Rh from the decay of ^{101}Pd does not allow an exact comparison.

The positive parity states are considered next and the presently available experimental information on the level structure of $^{99-105}$Rh is summarized in fig. 13b. The data are presented by referring the energies to the $\frac{9}{2}^+$ states which in the $^{95-105}$Rh isotopes lie at 64.6, 157.3, 93.1 and 19.5 keV above the $\frac{1}{2}^-$ state, respectively. These data are illustrated in this manner since by analogy with the $p_{\frac{1}{2}}$ coupled to the 2^+ state of the core, one would expect to observe a quintet with $\frac{5}{2}^+ \leqq J^\pi \leqq \frac{13}{2}^+$ resulting from the coupling of the $g_{\frac{9}{2}}$ quasiparticle to the 2^+ phonon state of the core at about the energy of the quadrupole excitation in neighboring doubly even nuclei. However, experimentally one finds that a $\frac{7}{2}^+$ state lies very close in energy to the $\frac{9}{2}^+$, and even below it in a number of cases, in the $Z = 43$, 45 and 47 nuclei [19]). Furthermore, in ^{99}Tc a $\frac{5}{2}^+$ state [19]) is lying very close to the $\frac{7}{2}^+$ and $\frac{9}{2}^+$ states, whereas in the Rh isotopes the $\frac{5}{2}^+$ and $\frac{7}{2}^+$ states are split by ≈ 300 keV and in the Ag isotopes by ≈ 600 keV. Since the QPC calculations for "spherical" nuclei as formulated by Kisslinger and Sorensen [9]) fail to account satisfactorily for the low-lying $\frac{5}{2}^+$ and $\frac{7}{2}^+$ states in N or $Z = 43$, 45, or 47 nuclei, several attempts have been made to extend and improve their coupling scheme. Ikegami and Sano [10]) have reported preliminary results of an expanded quasiparticle-phonon coupling scheme in which they include

admixtures from the next major shell (e.g. $d_{\frac{5}{2}}$, $g_{\frac{7}{2}}$, $s_{\frac{1}{2}}$ and $d_{\frac{3}{2}}$ from the Z or N 50–82 major shells). These authors find that their coupling scheme is effective in lowering the $\frac{5}{2}^+$ and $\frac{7}{2}^+$ relative to the $\frac{9}{2}^+$ and reported detailed calculations for the ^{77,79,81}Se isotopes.

The close occurrence of the single-quasiparticle and the phonon coupled levels was attributed by Sherwood and Goswami [11]) to the lifting of the quasiparticle levels due to coupling to backward going amplitudes. The extended quasiparticle-phonon coupling scheme (EQPC) of Sherwood and Goswami [11]) fails to account for the increasing energy difference between the $\frac{5}{2}^+$ and $\frac{7}{2}^+$ states as one goes from the Tc to the Ag isotopes. In a recent calculation Goswami and Nalcioglu [12]) used the measured [26]) quadrupole moments (large and negative) of the 2^+ states in the doubly even nuclei ^{104}Ru and ^{110}Pd to evaluate the quadrupole interaction matrix in their EQPC theory and they were thus able to account for the behavior of the $\frac{5}{2}^+$ and $\frac{7}{2}^+$ states. As can be seen in fig. 14 their calculations agree relatively well with the ^{101}Rh level sequence. In their calculations on ^{101}Rh Goswami and Nalcioglu [12]) used the value of -0.6 b for the quadrupole moment of the 2^+ state in ^{104}Ru which is probably larger than the quadrupole moment for ^{100}Ru. This can be inferred from the Coulomb excitation work of McGowan *et al.* [27]) who observed increased $B(\mathrm{E2}, 0^+ \rightarrow 2^+)$ values by a factor of 3.0 as one moves from ^{96}Ru to ^{104}Ru. However, if these authors had used a smaller value for the quadrupole moment of the ^{100}Ru core in their calculations for ^{101}Rh the agreement with experiment would be worse. Goswami and Nalcioglu [12]) have indicated from preliminary calculations that the inclusion of the two phonon levels is needed to get the correct level ordering.

It is interesting to point out the similarity in trend of the $\frac{7}{2}^+$, $\frac{5}{2}^+$ splitting with increased Z in going from Tc to Ag with the trend of the same splitting with increasing N in the Rh isotopes. In both cases the $\frac{7}{2}^+$, $\frac{5}{2}^+$ splitting appears to be increasing while the $\frac{7}{2}^+$ state appears to move down in energy relative to the $\frac{9}{2}^+$ state in a similar manner to the 2^+ state of the underlying core in the doubly even Ru isotopes. This trend should be predictable from the increasing quadrupole moment of the even mass Ru isotopes of the core.

Within the strict framework of the quasiparticle-phonon coupling models M1 transitions between members of coupled multiplets should be allowed (although hindered with E2 enhanced) and M1 transitions from the members of the multiplet to the single-quasiparticle states should be strictly forbidden. From our measurement of the total and K-shell conversion coefficients (table 3) for the 24.46 and 136.0 keV transitions ($\frac{7}{2}^+ \rightarrow \frac{9}{2}^+$) in ^{101}Rh and in ^{99}Rh, we estimated E2 admixtures of 3.8 ± 1.5 and 13 ± 4 %, respectively. These findings are contrary to the first order predictions of the phonon coupling model as discussed above. As it is seen in table 6 such E2 admixtures are typical in this region for transitions from members of the multiplet to the single-quasiparticle state for either the $g_{\frac{9}{2}}$ or the $p_{\frac{1}{2}}$ phonon coupled states. Whereas M1 transitions between the $\frac{3}{2}^-$ and $\frac{1}{2}^-$ levels in this region were explained by allowing small $p_{\frac{3}{2}}$ or $p_{\frac{1}{2}}$ single-quasiparticle admixtures to the phonon coupled

states, the corresponding $d_{\frac{5}{2}}$ and $g_{\frac{7}{2}}$ single-quasiparticle states lie very high above the $g_{\frac{9}{2}}$ and their admixture may be expected to be extremely small. However, as mentioned earlier from the work of Ikegami and Sano [10]) admixture from such higher lying states tends to lower the $\frac{5}{2}^+$ and $\frac{7}{2}^+$ states. If this description were applicable it would

TABLE 6

Experimental multipolarities and multipole mixing ratios of transitions in the odd mass Tc, Rh and Ag isotopes

Positive parity levels

Isotope	Transition [a])	E_γ(keV)	Multipolarity	Method of determination [b])
^{97}Tc	$\frac{7}{2}^+(1)\rightarrow\frac{9}{2}^+(1)$	215	M1+(6.7±6)% E2	α_K, K/L+M [33])
^{99}Tc	$\frac{7}{2}^+(1)\rightarrow\frac{9}{2}^+(1)$	141	M1+(7 ±3)% E2	α_K, K/L+M [45])
^{99}Rh	$\frac{7}{2}^+(1)\rightarrow\frac{9}{2}^+(1)$	136	M1+(13 ±4)% E2	α_K, K/L+M [c])
^{101}Rh	$\frac{7}{2}^+(1)\rightarrow\frac{9}{2}^+(1)$	25	M1+(3.8±1.5)% E2	α_T [c])
^{103}Rh	$\frac{7}{2}^+(1)\rightarrow\frac{9}{2}^+(1)$	53	M1+ < 1% E2	α_K, K/L [35, 36])
			M1+(13 ±2)% E2	α_K [37])
^{105}Rh	$\frac{9}{2}^+(1)\rightarrow\frac{7}{2}^+(1)$	149	M1+(19 ±8)% E2	α_L [38])
^{109}Ag	$\frac{9}{2}^+(1)\rightarrow\frac{7}{2}^+(1)$	45	M1+ 16 % E2	α_T [29])
^{99}Tc	$\frac{5}{2}^+(1)\rightarrow\frac{7}{2}^+(1)$	41	M1	α_K [34])
	$\frac{3}{2}^+(1)\rightarrow\frac{5}{2}^+(1)$	740	M1 and/or E2	α_K [45])
^{99}Rh	$\frac{5}{2}^+(1)\rightarrow\frac{7}{2}^+(1)$	264	M1+(17 ± 10)% E2	α_K [c])
^{101}Rh	$\frac{5}{2}^+(1)\rightarrow\frac{7}{2}^+(1)$	296	M1+(16 ± 8)% E2	α_K [c])
^{103}Rh	$\frac{5}{2}^+(1)\rightarrow\frac{7}{2}^+(1)$	497	M1 and/or E2	α_K [39])
^{105}Rh	$\frac{5}{2}^+(1)\rightarrow\frac{7}{2}^+(1)$	469	M1 and/or E2	α_K [38])
^{107}Ag	$\frac{5}{2}^+(1)\rightarrow\frac{7}{2}^+(1)$	829	M1 and/or E2	α_K [40])
^{101}Rh	$\frac{7}{2}^+(2)\rightarrow\frac{5}{2}^+(1)$	270	M1+(10 ±5)% E2	α_K [c])
^{103}Rh	$\frac{7}{2}^+(2)\rightarrow\frac{7}{2}^+(1)$	610	M1 and/or E2	α_K [39])
^{105}Rh	$\frac{7}{2}^+(2)\rightarrow\frac{7}{2}^+(1)$	499	M1 and/or E2	α_K [38])
^{103}Rh	$\frac{3}{2}^-(1)\rightarrow\frac{1}{2}^-(1)$	295	M1+(2.8±3)% E2	Coul. Excit. $\gamma(\theta)$ [41])
			M1+(37 ± 35)% E2	α_K [36, 42, 43])
^{105}Rh	$\frac{3}{2}^-(1)\rightarrow\frac{1}{2}^-(1)$	263	M1	α_K [38])
^{107}Ag	$\frac{3}{2}^-(1)\rightarrow\frac{1}{2}^-(1)$	325	M1+(4.2±0.4)% E2	Coul. Excit. $\gamma(\theta)$ [41])
^{109}Ag	$\frac{3}{2}^-(1)\rightarrow\frac{1}{2}^-(1)$	309	M1+(3.5±0.4)% E2	Coul. Excit. $\gamma(\theta)$ [41])
^{103}Rh	$\frac{5}{2}^-(1)\rightarrow\frac{3}{2}^-(1)$	62	M1+ < 2% E2	α_L [42])
^{107}Ag	$\frac{5}{2}^-(2)\rightarrow\frac{5}{2}^-(1)$	720	M1 and/or E2	α_K [40])
			M1 + 45% E2	$\gamma\gamma(0)$ [44])

[a]) The number in parentheses gives the number of the level with this J^π value.

[b]) The theoretical conversion coefficients from ref. [17]) have been used to calculate the E2 admixtures. The data on α_K and K/(L+M) ratios are from the references given.

[c]) From this work, see also footnote [b]) in table 3.

accomplish (i) the lowering of the phonon coupled states of Goswami and Nalcioglu closer to the corresponding experimental levels, and (ii) would allow for the M1 transition between members of the multiplet and the quasiparticle state.

The E2 admixture for the ($\frac{5}{2}^+ \rightarrow \frac{7}{2}^+$) 296.24 keV transition is 16 ± 8 % which is consistent with the QPC model. However the ($\frac{7}{2}^{+\prime} \rightarrow \frac{5}{2}^+$) 269.66 keV transition which is presumably between a two-phonon coupled state and one-phonon coupled state has a 10 ± 5 % E2 admixture which again may require some single quasiparticle admixture to either state in order to explain the M1 transition probability.

The $\frac{11}{2}^+$ and $\frac{13}{2}^+$ members of the proposed quintet are predicted to lie very low by the EQPC theory [12]) but such states have not been observed in the Tc or Rh isotopes. However, Berzins *et al.* [28]) have observed two states in ^{111}Ag from the decay of the $\frac{11}{2}^-$ isomer of ^{111}Pd at 575 and 1028 keV above the $\frac{9}{2}^+$ state which are candidates for the $\frac{11}{2}^+$ and $\frac{13}{2}^+$ states, respectively. However, this does not agree with the calculations of Goswami and Nalcioglu [12]) for the analogous states in ^{109}Ag which are expected at 110 keV below and 250 keV above the $\frac{9}{2}^+$, respectively.

As mentioned by Graeffe and Gordon [29]) the $g_{\frac{9}{2}}$ orbital in the 28–50 neutron shell is analogous to the $h_{\frac{11}{2}}$ orbital in the 50–82 neutron shell; these are high-spin orbitals of the given parity lying close in energy to several low spin levels of opposite parity. According to Kisslinger [30]), when the opposite parity orbitals are about half full the (j–1) member of a three-quasiparticle configuration may occur at very low energy. This appears to be the case in the 50–82 neutron shell since the $\frac{9}{2}^-$ level exists [19]) at about 200 keV above the $\frac{11}{2}^-$ isomer in ^{125,127}Te. This analogy leads one to expect that the lowest $\frac{7}{2}^+$ state could be described as the (j–1) state of a three-quasiparticle configuration. In this respect, Graeffe and Gordon [29]) have pointed out that whereas the $\frac{9}{2}^- \rightarrow \frac{11}{2}^-$ transitions in the Te isotopes had large E2/M1 mixing ratios this was not the case for the $\frac{7}{2}^+ \rightarrow \frac{9}{2}^+$ transitions in ^{103}Rh. Since that time, however, new experimental information has become available (see table 6) to support the fact that the E2/M1 mixing ratios for these transitions in the odd-mass Tc, Rh and Ag isotopes are of the same order of magnitude with the mixing ratios for the $\frac{9}{2}^- \rightarrow \frac{11}{2}^-$ transition [31]) in ^{125}Te. In connection to this, it may be interesting to note that Kownacki *et al.* [32]) measured the half-life of the $\frac{9}{2}^-$ state in ^{125}Te and using the value [13]) of 28 % for the E2 admixture in the $\frac{9}{2}^- \rightarrow \frac{11}{2}^-$ transition they calculated $B(\mathrm{E2})_{\mathrm{exp}}/B(\mathrm{E2})_{3\mathrm{q.p.\,theor.}} = 1.09 \pm 0.05$ and $B(\mathrm{M1})_{\mathrm{s.p.}}/B(\mathrm{M1})_{\mathrm{exp}} = 275$ for the E2 enhancement and M1 retardation factors over the three-quasiparticle [30]) and single-proton estimates, respectively. Unfortunately, the half-lives of the lowest $\frac{7}{2}^+$ states in the Tc, Rh and Ag isotopes are not known for those transitions for which reasonable estimates of the E2/M1 mixing ratios exist. Such measurements together with more accurate results on the mixing ratios will be needed before a clear selection between the various descriptions that have been put forth can be made.

We wish to thank Mr. John Hood and the personnel of the Washington University cyclotron for performing the bombardments. The continued cooperation of Dr. T. Gallagher and the staff of the Washington University computing facilities is appreciated. We thank Dr. M. Ter-Pogossian for the use of the Si(Li) X-ray spectrometer.

References

1) M. Lindner and I. Perlman, Phys. Rev. **73** (1948) 1202
2) D. T. Eggen and M. L. Pool, Phys. Rev. **75** (1949) 1464
3) S. Katcoff and H. Abrash, Phys. Rev. **103** (1956) 966
4) K. S. Thorne and E. Kashy, Nucl. Phys. **60** (1964) 35
5) Nuclear Data Sheets, NRC 61-2-26
6) B. S. Dzhelepov, N. M. Antoneva, M. K. Nikitin and V. B. Smirnov, JETP (Sov. Phys.) **10** (1965) 20
7) J. S. Evans, E. Kashy, R. A. Naumann and R. F. Petry, Phys. Rev. **138** (1965) B9
8) M. E. Phelps and D. G. Sarantites, Nucl. Phys. **A135** (1969) 116
9) L.S. Kisslinger and R. A. Sorensen, Rev. Mod. Phys. **35** (1963) 853
10) H. Ikegami and M. Sano, Phys. Rev. Lett. **21** (1966) 323
11) A. I. Sherwood and A. Goswami, Nucl. Phys. **89** (1966) 465
12) A. Goswami and O. Nalcioglu, Phys. Lett. **26B** (1968) 353
13) M. E. Phelps, D. G. Sarantites and W. G. Winn, Nucl. Phys. **A149** (1970) 647
14) W. G. Winn and D. G. Sarantites, Nucl. Instr. **66** (1968) 61
15) W. G. Winn and D. G. Sarantites, Phys. Rev. **184** (1969) 1188
16) International Atomic Energy Agency, Vienna, Jan. 1970
17) R. S. Hager and E. C. Seltzer, Nucl. Data, **A4** (1968) 1;
R. F. O'Connell and C. O. Carroll, Nucl. Data, **A3** (1967) 287
18) J. S. Evans and R. A. Naumann, Phys. Rev. **140** (1965) B559
19) C. M. Lederer, J. M. Hollander and I. Perlman, Table of isotopes, sixth ed. (Wiley, New York, 1967)
20) B. Cujec, Phys. Rev. **131** (1963) 735
21) I. Lindgren, Table of nuclear spins and moments, in Alpha-, beta and gamma-ray spectroscopy, Appendix 4, ed. K. Siegbahn (North-Holland, Amsterdam, 1964)
22) M. E. Phelps, A. Friedman and D. G. Sarantites, unpublished results (1970);
H. E. Phelps, Ph. D. thesis, Washington University (1970), unpublished
23) A. de-Shalit, Phys. Rev. **122** (1961) 1530
24) R. D. Lawson and J. L. Uretzky, Phys. Rev. **108** (1957) 1300
25) J. L. Black, W. J. Caelli and R. B. Watson, Nucl. Phys. **A125** (1969) 545
26) P. H. Stelson, in Proc. of the summer study groups in the physics of the Emperor tandem Van de Graaff Region, Vol. III, p. 1005, Brookhaven National Laboratory (1965)
27) F. K. McGowan, R. L. Robinson, P. H. Stelson and W. T. Milner, Nucl. Phys. **A113** (1968) 529
28) G. Berzins, M. E. Bunker and J. W. Starner, Nucl. Phys. **A126** (1969) 273
29) G. Graeffe and G. E. Gordon, Nucl. Phys. **A107** (1967) 67
30) L. S. Kisslinger, Nucl. Phys. **78** (1966) 341
31) E. P. Magee and Yu. W. Sergiejenkow, Izv. Akad. Nauk SSSR (ser. fiz.) 30 (1966) 1237
32) J. Kownacki, J. Ludziejewski and M. Moszyński, Nucl. Phys. **A113** (1968) 561
33) G. Graeffe, Nucl. Phys. **A127** (1969) 65
34) N. Ranakumar, R. W. Fink and P. Venugopala Rao, Nucl. Phys. **A127** (1969) 683
35) V. R. Potnis, E. B. Nieshmidt, C. E. Mandeville, L. D. Ellsworth and G. P. Agin, Phys. Rev. **146** (1966) 883
36) J. C. Manthuruthil, H. J. Hennecke and C. R. Cothern, Phys. Rev. **165** (1968) 1363
37) A. Mukerji, D. N. McNelis and J. W. Kane Jr., Nucl. Phys. **67** (1965) 466
38) S. O. Schriber and M. W. Johns, Nucl. Phys. **A96** (1967) 337
39) W. H. Zoller, E. S. Macias, M. B. Perkal and W. B. Walters, Nucl. Phys. **A130** (1969) 293
40) N. L. Lark, P. F. A. Goudsmit, J. F. Jansen, J. E. J. Oberski and A. H. Wapstra, Nucl. Phys. **35** (1962) 582
41) F. K. McGowan and P. H. Stelson, Phys. Rev. **109** (1958) 901
42) Y. Grunditz, S. Antman, H. Petterson and M. Saraceno, Nucl. Phys. **A133** (1969) 369
43) D. E. Raeside, J. J. Reidy and M. L. Wiedenbeck, Nucl. Phys. **A134** (1969) 347
44) J. L. Black and W. Gruhle, Nucl. Phys. **A93** (1967) 1
45) C. W. E. Van Eijk, B. Van Nooijen, F. Schutte, S. M. Brahmavar, J. H. Hamilton and J. J. Pinajian, Nucl. Phys. **A121** (1968) 440